AALBORG UNIVERSITY

DENMARK

Earthquake Tests on Midbroken Scale 1:5 Reinforced Concrete Frames

Skjærbæk, P. S.; Nielsen, Søren R. K.; Kirkegaard, Poul Henning; Taskin, B

[Link to publication from Aalborg University](#)

P.S. SKJÆRBÆK, S.R.K. NIELSEN, P.H. KIRKEGAARD, B. TAŞKIN
EARTHQUAKE TESTS ON MIDBROKEN SCALE 1:5 REINFORCED CON-
CRETE FRAMES

Earthquake Tests on Midbroken Scale 1:5 Reinforced Concrete Frames

P.S. Skjærbæk, S.R.K. Nielsen and P.H. Kirkegaard
Department of Building Technology and Structural Engineering,
Aalborg University, DK-9000 Aalborg, Denmark

B. Taşkın
Department of Structural Engineering,
İstanbul Technical University, 80626 Maslak, İstanbul, Turkey

Contents

Chapter 1

Introduction

Dynamic loads seen in the nature such as earthquakes, wind, flood, and etc. causes damages in civil engineering structures. Since there is no escape from this reality, the only thing that can be done for an excisting structure is to control the damage growth by suitable localization and quantification procedures. In most earthquake codes, the acceptable degrees of expected damage changes according to the strength of an earthquake, but the main idea is to prevent the total collapse of a structure or total collapse of a part of a structure and make it repairable, so the demolition of the structure will be avoided. This point of view led to a new research area known as "damage assessment" resulting in the recent 10-20 years in many different methods in the literature.

In reinforced concrete, (RC), structures, damage under dynamic loadings usually starts as cracks followed by crushing of concrete or yielding of reinforcement, in case the structure does not suffer any other kind of construction failure. Traditionally assessment of damage in RC-structures, is done by visual inspection of the structure by measuring cracks, permanent deformations, etc. This is often very cumbersome, since panels and other walls covering beams and columns need to be removed. But developments in earthquake engineering and especially developments in the recent 10-20 years of damage assessment procedures, offers a much more attractive method which basicly depends on measuring the structural response at given locations of the structure. Almost all of the methods developed according to this idea are based on calculating a socalled damage index, which is supposed to reflect the damage state of the considered structure, substructure or structural member by the use of e.g. changes in dynamic characteristics. In the literature, several methods for damage assessment from measured responses have been presented during the last 2 decades, see Banon et al. [1] Stubbs et al. [44], Penny et al., [30], Casas [6], DiPasquale et al. [8], Hassiotis et al. [12], Koh et al. [18], Pandey et al. [25], Park et al. [26], [27] , Penny et al. [30], Reinhorn et al. [31], Rodriguez-Gomes [32], Skjærbæk et al., [39], [37], Stephens et al. [42], [43] and Vestroni et al. [46].

Recent earthquake events have revealed a class of structures which can be referred as mid-broken structures. (Pan Cake type of damage). As a definition a mid-broken structure has a storey weakened by some kind of changes in the material used or changes of the geometry of members' cross-sections. Examples of this phenomenon are found in Turkey and Greece, where buildings are often built in several stages. After the construction of each stage, reinforcement bars are left extended through the next and finally through the concrete deck at the roof. When construction work is resumed, perhaps years later these extended reinforcement bars are used to connect and anchroge the new stuctural components to the existing building. Recent

earthquake events in Turkey and Greece have shown that such mid-broken structures have a tendency of failing in the storeys where such a connection is performed. The same kind of failure mode was also seen in the Kobe 1995 earthquake, where the mid-storey collapses were caused by a sudden change of stiffness and strenght of the storey columns.

An example of such a failure can be seen in Figure 1.1 below.
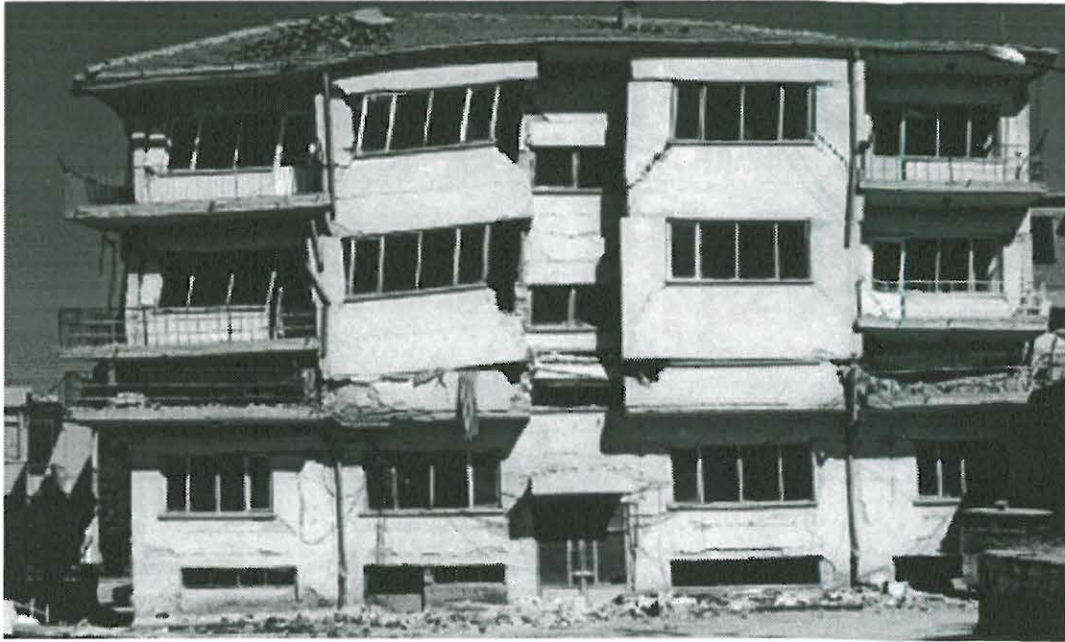
Figure 1.1: Collapse of an intermedia floor due to the October 1995 Earthquake, Dinar, Turkey.

Until now only very limited research have been dedicated to this phenomenon, and the studies have been limited to numerical simulation studies by e.g. Skjærbæk et al.[40], and Köylüoğlu et al. [19], [20]. The results of these simulations indicate that the increased amount of damage in a weak storey, is mainly due to the strength degradation. However, some divergency has been found between different models used in the simulations and experimental verification of the simulated results are desired.

The aim of this report is to present the results of a shaking table experiment with such a structure, where the reinforcement have been weakened in the fourth storey.

The report is organized so that chapter 2 define the structure including the results from the material testing performed. In chapter 3 the test set-up and the conduction of the dynamic tests are explained for both non-destructive and destructive testing. Chapters 4 present the results of the non-destructive testing and chapter 5 results from the destructive strong motion experiments. In chapter 6 it is defined how various static tests with the structure are performed and the results from these static tests of the reference frame as well as the damaged frame are presented. Finally chapter 7 presents the results of the visual inspections performed during the destructive strong motion experiments. Appendix A contains photos taken during the process from casting of the frames until the static testing.

Chapter 2

Definition of the test structure

For the test series 3 reinforced concrete frames were casted one at a time. For each frame casting reference specimens were casted for determination of compression strength of the concrete used for each of the frames. In the following the design specifications of the frames and the reference specimens are described.

2.1 Frame structure

All the 3 frames considered in the test series were constructed identically. The test frame considered is a 6-storey, 2 bay RC-frame. The dimensions of the test frame is 2400 by 3300 mm. Corresponding to a "real" structure with dimensions 12 by 16.5 m. The test frame is build of 50 by 60 mm RC-sections reinforced with 6 mm KS550 (EU-code name) and St37 (EU-code name). A plane view of the test frame is shown in figure 2.1. The weight of each frame is ≈ 2 kN. To model the storey deck, 8 RC beams (0.12*0.12*2.0m) are placed on each storey. The total weight per frame is then ≈ 20 kN.

2.1.1 Reinforcement

The longitudinal reinforcement used in the frame are of the type KS550 (ribbed steel) with an average yield stress of 610 MPa. In the weak storey St37 steelbars were used with an average yield strenght of 390 MPa. In figures 2.2 and 2.3 the stress-strain curves for the two types of steel are shown.
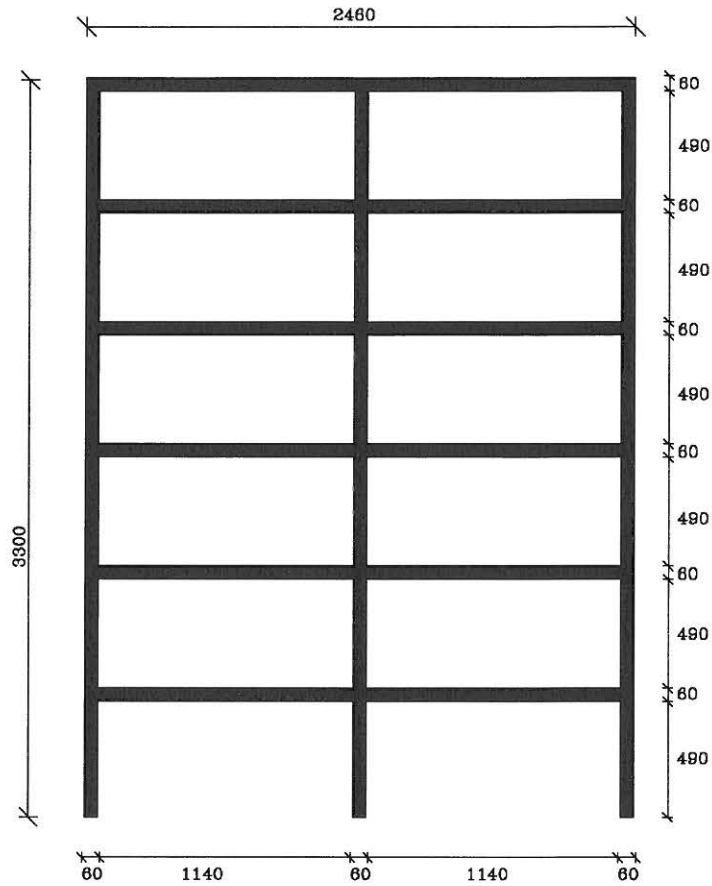
Figure 2.1: Plane view of test frames.
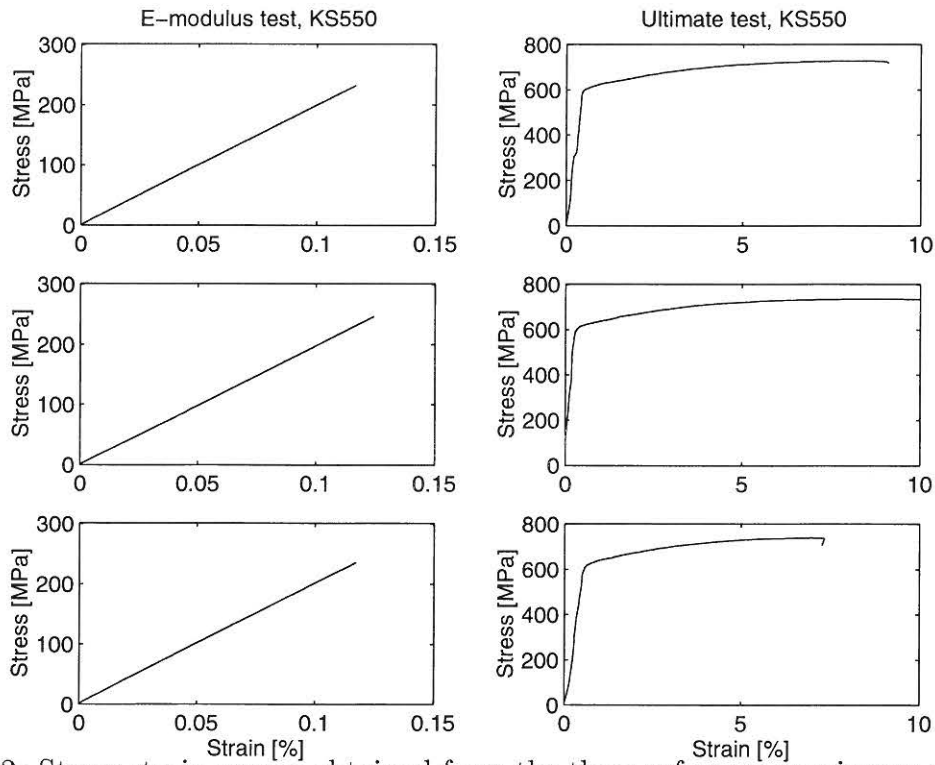
Figure 2.2: Stress-strain curves obtained from the three reference specimens of the used KS550 reinforcement bars.
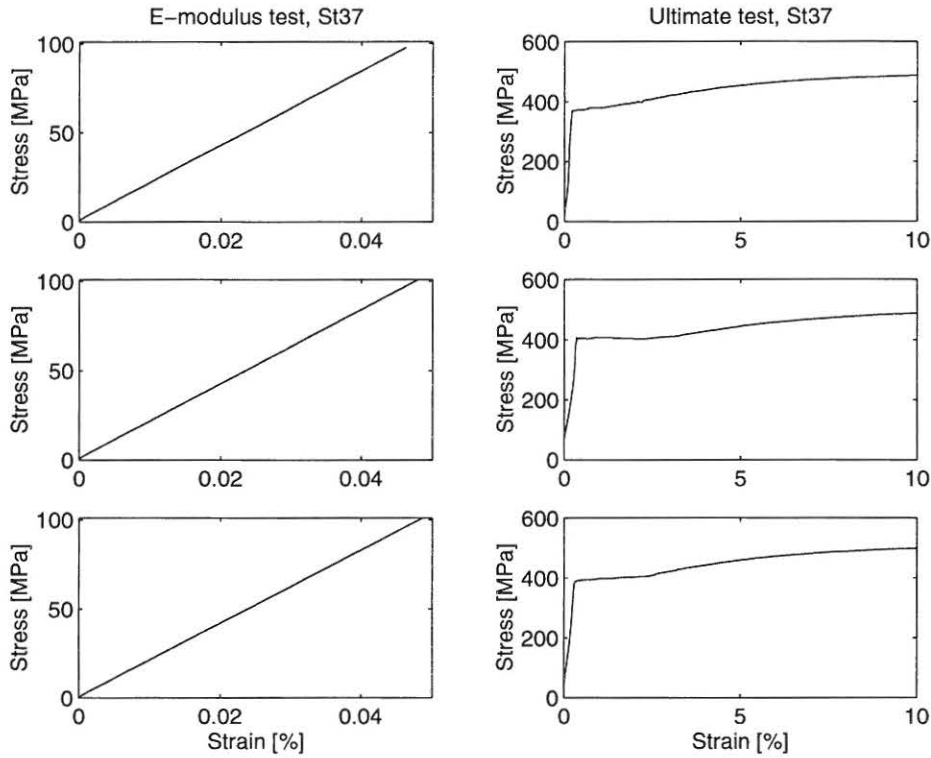
Figure 2.3: Stress-strain curves obtained from the three reference specimens of the used st37 reinforcement bars.

In tables 2.1 and 2.2 the evaluated yield stresses, f_{sy}, ultimate stresses, f_{su}, and modulus of elasticity E_s for the two types of steel are shown.

Specimen	f_{sy} [MPa]	f_{su} [MPa]	E_s [$\frac{10^5 \text{N}}{\text{m}^2}$]
1	590	725	1.983
2	600	735	1.979
3	615	740	1.991

Table 2.1: *Determined characteristics of the longitudinal reinforcement, KS550.*

To evaluate the performed stuk-welding between the two types of reinforcement, three reference specimens were constructed and tested like an ordinary reinforcement bar. The obtained stress-strain curve are illustrated in figure 2.4.

To avoid overlapping longitudinal reinforcement giving changing bending stiffness and strength the longitudinal reinforcement bars are ended with anchoring steel-plates welded to the reinforcement.

2.1.2 Concrete

The concrete used has a design cylindrical compression strength of 30 MPa with a maximum aggregate diameter of 5 mm. For each frame is used approximately 80 l concrete. For each frame three reference concrete cylinders was casted and modulus of elasticity and maximum compression strenght were evaluated. The results of the tests for the three frames are shown in table 2.3.

Specimen	f_{sy} [MPa]	f_{su} [MPa]	E_s [$\frac{10^5 \mathrm{N}}{\mathrm{m}^2}$]
1	370	480	2.089
2	405	490	2.080
3	385	505	2.056

Table 2.2: *Determined characteristics of the longitudinal reinforcement, St37.*
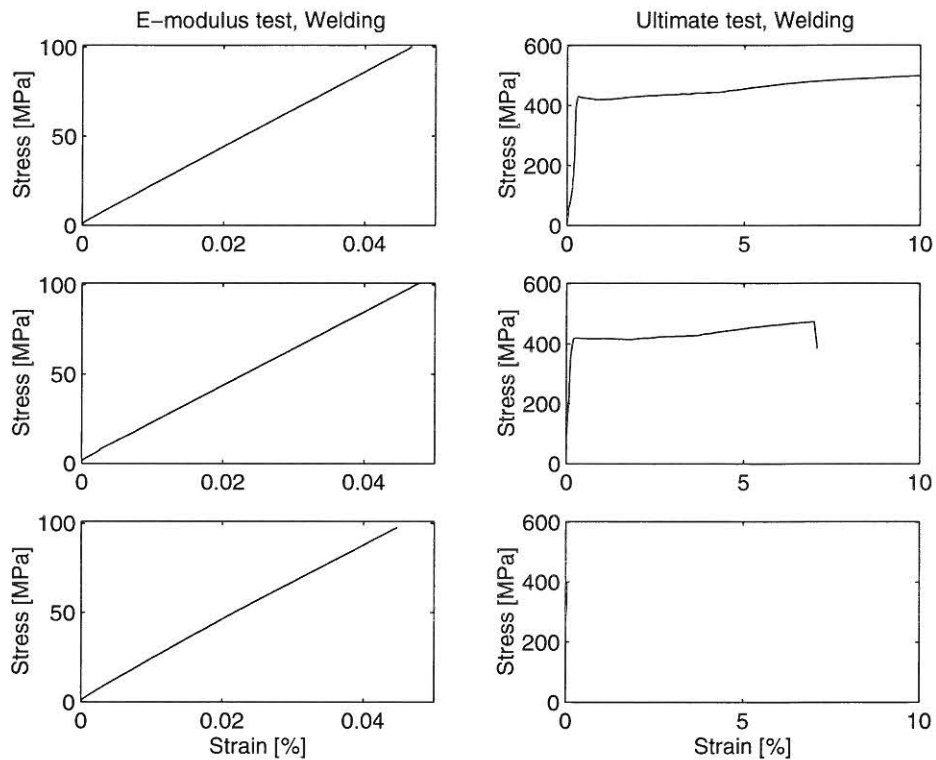
Figure 2.4: Stress-strain curves obtained from the three reference specimens of the welded connection between KS550 and St37.

2.1.3   Shear reinforcement

All cross-sections are reinforced for shear with 2mm steel thread which has been twisted around the longitudinal reinforcement into spirals, see figure 2.5. The characteristic tension strength is 235 MPa, and the distance between the loops is approximately 20 mm.

2.1.4   Beams and columns

The dimensions of the beams and columns in the frame are constant all over the frame with outer measures of 50 × 60 mm. Columns and beams are reinforced with 4ø6 KS550 (ribbed steel), see figure 2.6a. The columns in the weak fourth storey are reinforced with 4ø5.5 St37 reinforcement bars as illustrated in figure 2.6b.

Specimen	f_c [MPa]	E [MPa]
AAU-W1-1	42.5	-
AAU-W1-2	41.5	29300
AAU-W1-3	41.3	29800
AAU-W2-1	44.0	-
AAU-W2-2	46.2	34000
AAU-W2-3	41.1	32500
AAU-W3-1	47.1	-
AAU-W3-2	41.2	29000
AAU-W3-3	43.0	26000

Table 2.3: *Determined characteristics from the reference concrete cylinders.*
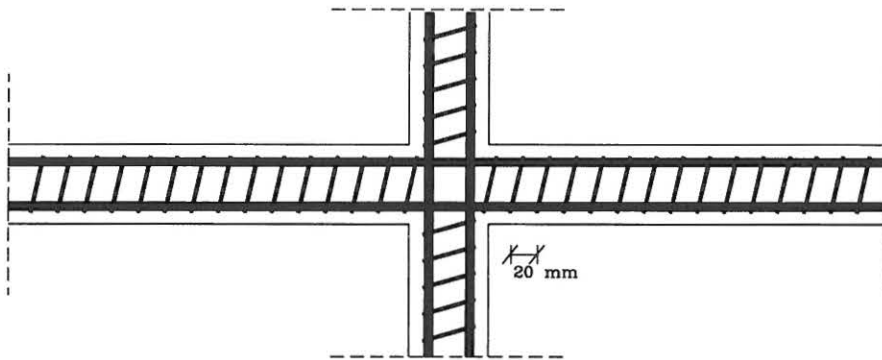
Figure 2.5: Shear reinforcement of columns and beams.
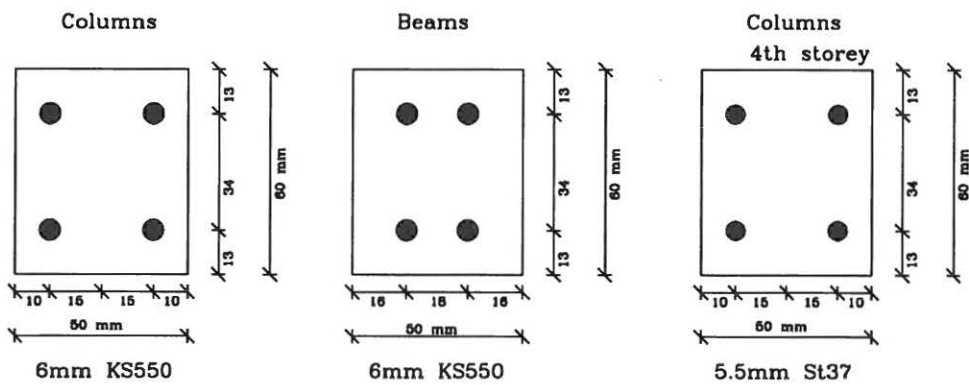
Figure 2.6: Cross-section of beam and columns.

Chapter 3

Test set-up and conduction of dynamic tests

3.1 S⎯⎯king table

The sh⎯king table is constructed of two frames of HEB 160 steel profile. The two frames are connec⎯ed by two linear leaders with a dynamic carring capacity of 9000 N per carriager. The force i⎯ produced by a 63 kN HBM cylinder with a ±20 mm displacement field. A schematic view ⎯f the shaking table is shown in figure 3.1.
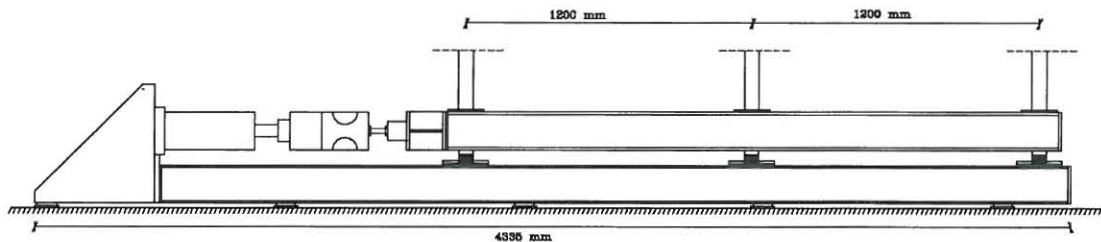
Figure 3.1: Dimensions of shaking table.

3.2 Experimental set-up

The frames are tested in pairs of two where the same ground surface acceleration is applied to the two frames. The frames are placed at the shaking table at a distance of 1000 mm and is stabilized in space by steel crosses at each end.
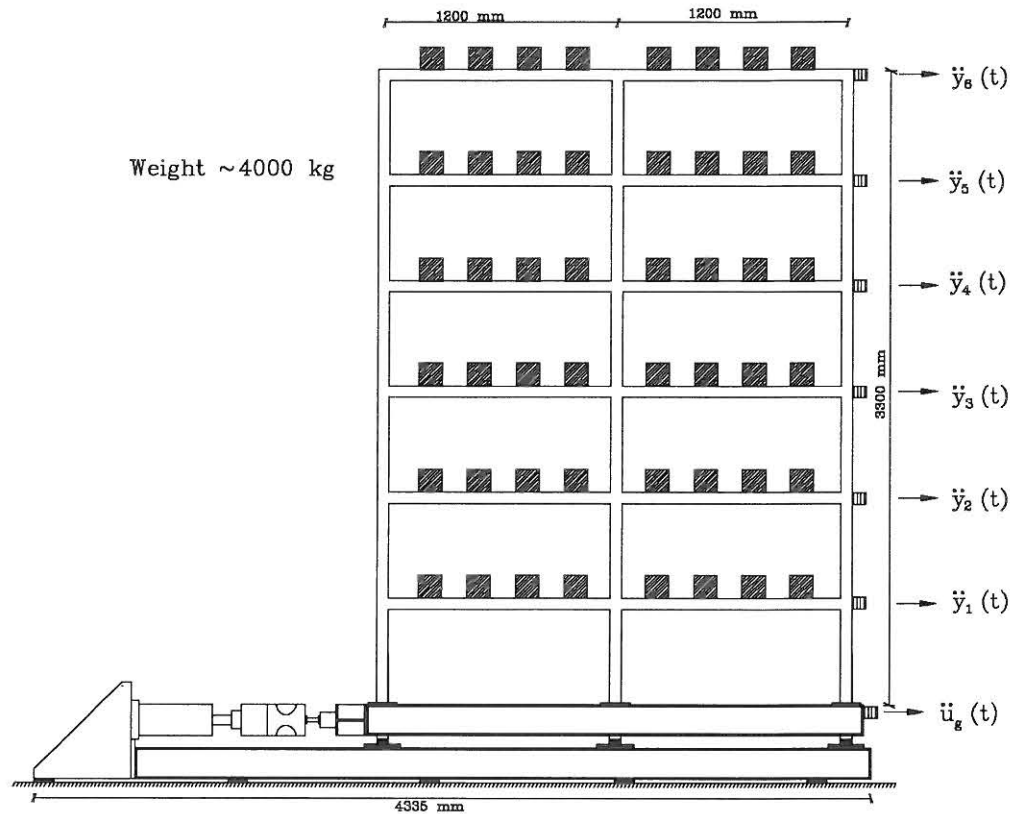
Figure 3.2: Side view of experimental set-up.

The hydraulic cylinder providing the base motions is controlled by a HBM computer system. In the connection between the shaking table and the hydraulic cylinder a load cell is placed to measure the actual cylinder force as a function of time. Furthermore, the cylinder is capable of measuring the cylinder displacements as function of time.

3.2.1 Free Decay Tests

Free decay tests with the frames were for the frame AAUW performed by applying a horizontal force at the top storey of the frame. A load-cell was used to measure the pull-out force, see figure 3.3.
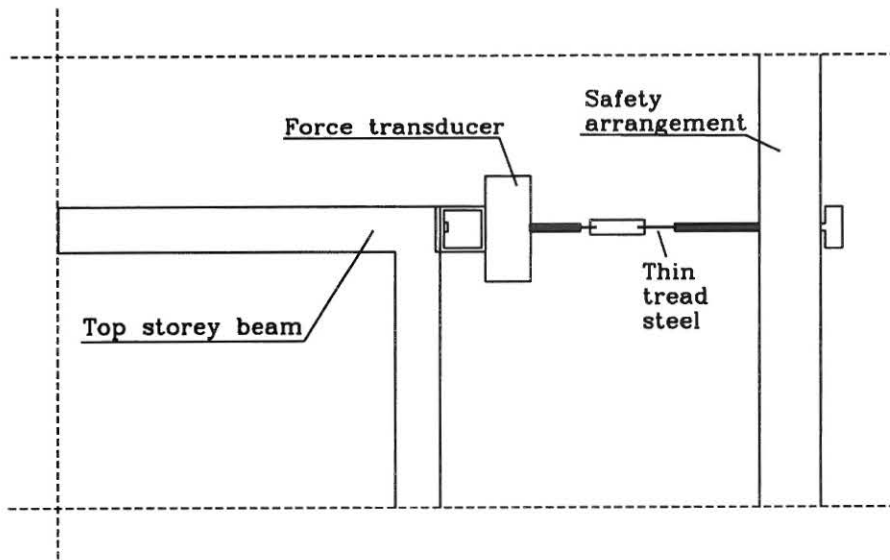
Figure 3.3: Pull out arrangement used for free decay tests.

3.2.2 Instrumentation of frame

Both the right and left frame were equipped with an accelerometer measuring the horizontal acceleration. The exact location of the measuring devices on the frame are shown in figures 3.4 and the number and type of transducers are shown in table 3.1.
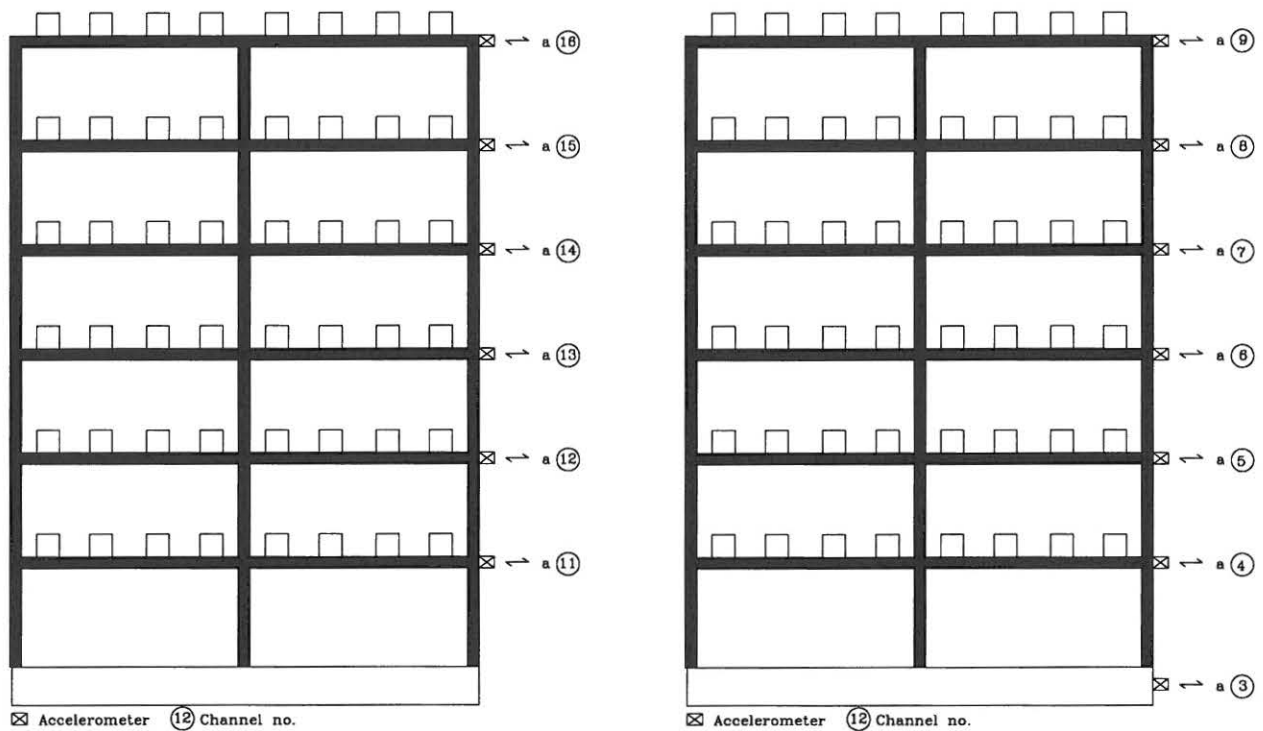
Figure 3.4: Instrumentation of the right and left frame for set-up AAUW.

Channel	Response	Type	Calibration
1	Force	HBM	10V=63kN
2	Displacement	HBM	10V=20 mm
3	Acceleration	BK8306	9.86 V/g
4	Acceleration	BK8306	9.80 V/g
5	Acceleration	BK4370	1.00 V/ms^{-2}
6	Acceleration	BK4370	1.00 V/ms^{-2}
7	Acceleration	BK4370	1.00 V/ms^{-2}
8	Acceleration	BK4370	1.00 V/ms^{-2}
9	Acceleration	BK4370	1.00 V/ms^{-2}
10	-	-	-
11	Acceleration	K8304B2	1027 mV/g
13	Acceleration	K8304B2	963 mV/g
14	Acceleration	K8304B2	956 mV/g
12	Acceleration	K8304B2	1008 mV/g
15	Acceleration	K8304B2	963 mV/g
16	Acceleration	K8304B2	963 mV/g

Table 3.1: *The used transducers and calibration factors. BK=Brüel & Kjær, K=Kistler.*

3.2.3   Data aquisition system

All transducers are connected to a 16-channel HBM data acquisition system where data from all channels are sampled simultaneously with a rate of 150 Hz.

Chapter 4

Non-destructive dynamic testing

In this chapter the results of the non-destructive testing of the frame in the virgin state and the results after each strong motion event are presented. Before strong motions are applied the frame is subjected to various loadings in the linear range to provide data for modal identification of the original structure. Furthermore, free decay tests are performed after each earthquake to provide "clean" data for identification of the damaged structure.

The original frame is subjected to free decays from pull-outs in bending of 0.25 kN, 0.50 kN and 0.75 kN.

The name of the files for the frame are shown in table 4.1.

Name	Case
fd4_b01.dat	Free decay (virgin), Pull-out force of 0.25 kN.
fd4_b02.dat	Free decay (virgin), Pull-out force of 0.50 kN.
fd4_b03.dat	Free decay (virgin), Pull-out force of 0.75 kN.
fd4_b04.dat	Free decay (virgin), Pull-out force of 0.25 kN.
fd4_b05.dat	Free decay (before strong motion), Pull-out force of 0.25 kN.
fd4_b06.dat	Free decay (after EQ1), Pull-out force of 0.25 kN.
fd4_b07.dat	Free decay (after EQ1), Pull-out force of 0.50 kN.
fd4_b08.dat	Free decay (after EQ1), Pull-out force of 0.75 kN.
fd4_b09.dat	Free decay (before strong motion), Pull-out force of 0.50 kN.
fd4_b10.dat	Free decay (after EQ2), Pull-out force of 0.25 kN.
fd4_b11.dat	Free decay (after EQ2), Pull-out force of 0.50 kN.
fd4_b12.dat	Free decay (after EQ2), Pull-out force of 0.75 kN.
fd4_b13.dat	Free decay (before strong motion), Pull-out force of 0.50 kN.
fd4_b14.dat	Free decay (after EQ3), Pull-out force of 0.25 kN.
fd4_b15.dat	Free decay (after EQ3), Pull-out force of 0.50 kN.
fd4_b16.dat	Free decay (after EQ3), Pull-out force of 0.75 kN.

Table 4.1: *File names for the data from non-destructive testing of frame AAUW in the virgin state and after each earthquake.*

4.1 Data Processing

All data presented in this chapter are detrended by removing the best straight line in order to remove any trends in the signals. Furthermore low-pass filtering have been performed using a 8th order Butterworth digital filter with a cut-off frequency of 11 Hz.

4.2 Non-destructive dynamic testing of frame

In this section some selected results of the non-destructive tests are shown for frame AAUW.

4.2.1 Free decay tests

Figure 4.1: Measured accelerations from pull-out test of undamaged frame AAUW. Pull-out force of 0.5 kN.

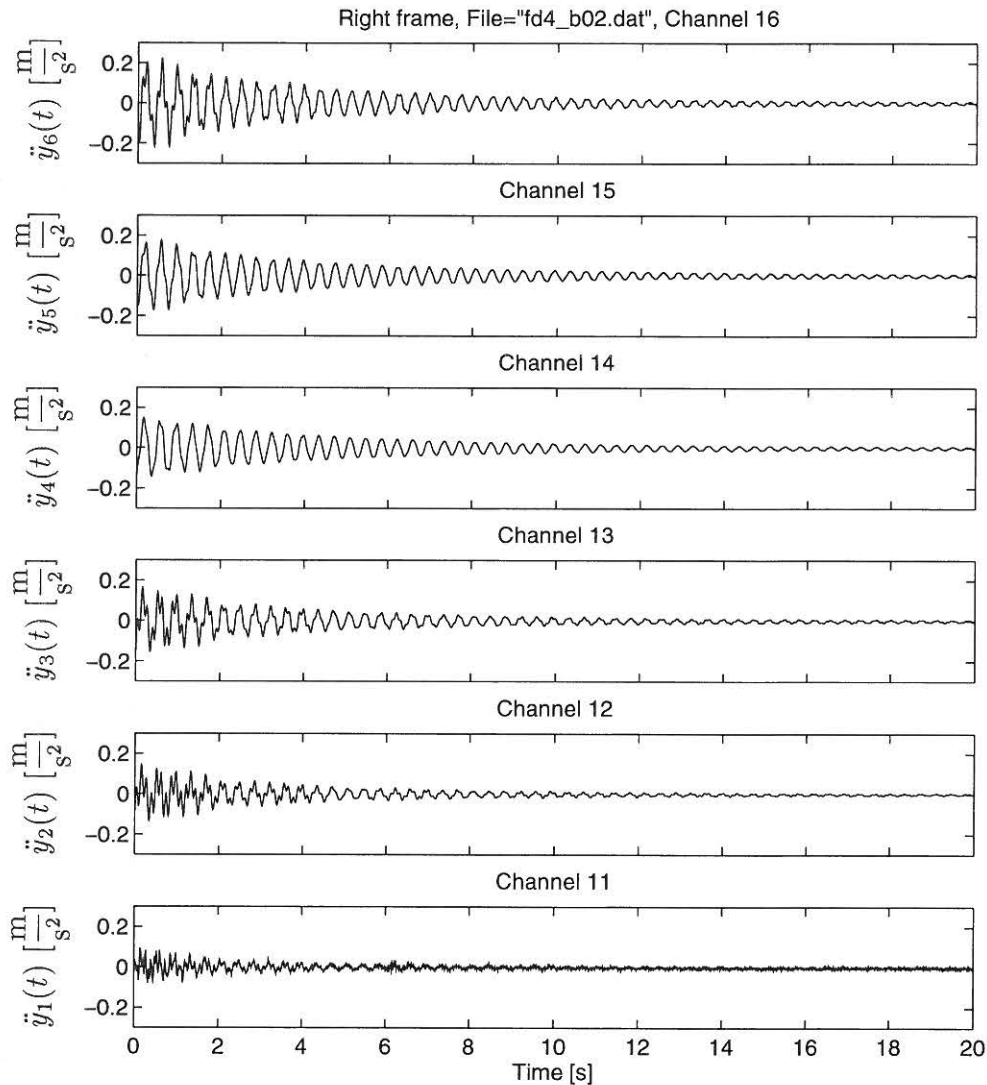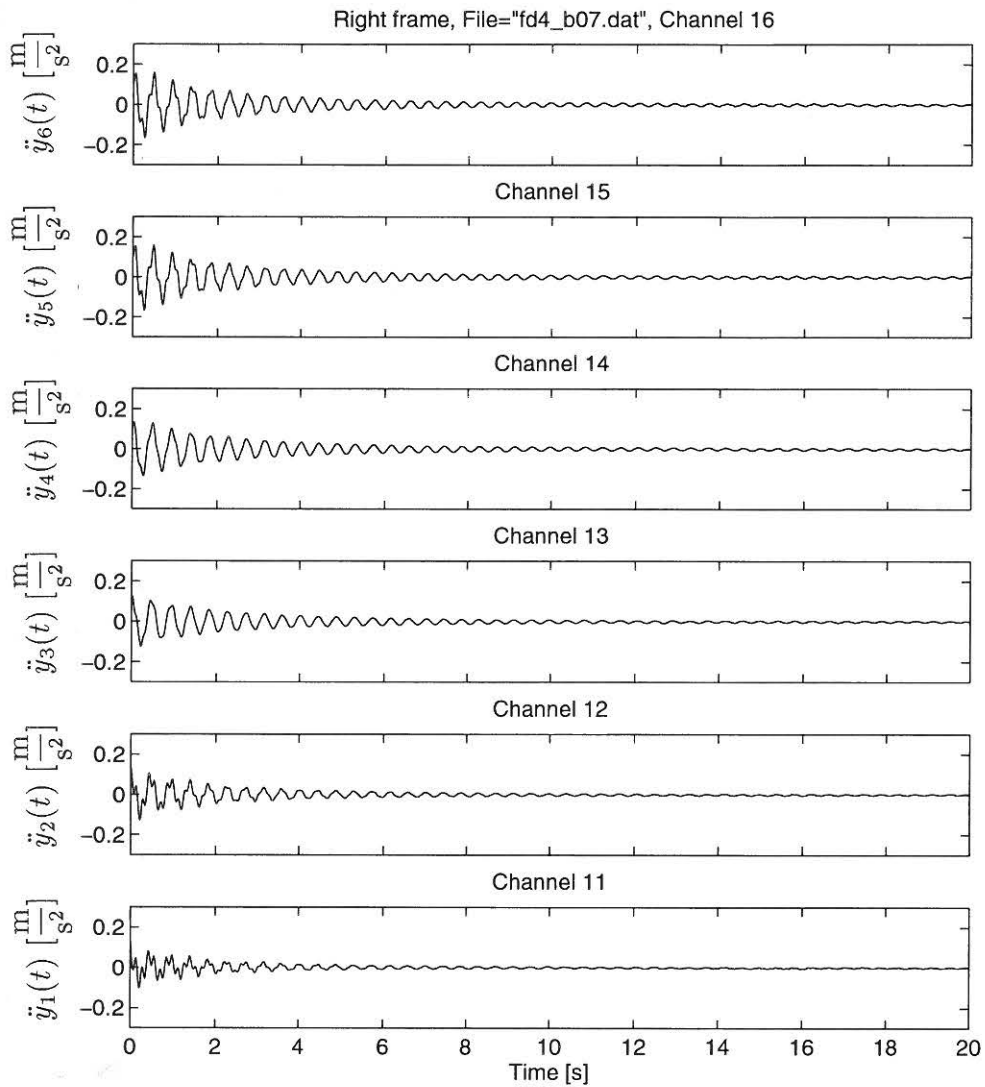Right frame, File="fd4_b07.dat", Channel 16

Figure 4.2: Measured accelerations from pull-out test of frame AAUW after EQ1. Pull-out force of 0.5 kN.
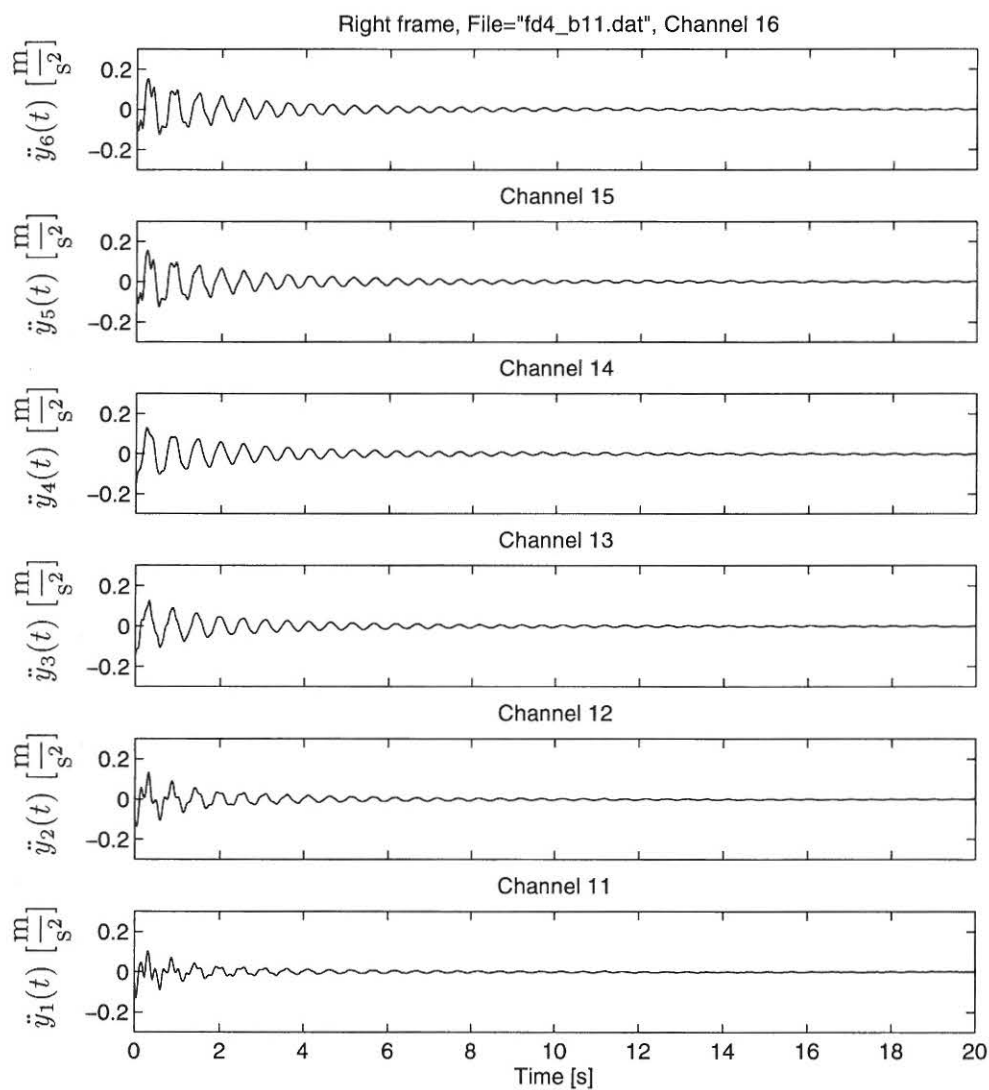
Figure 4.3: Measured accelerations from pull-out test of frame AAUW after EQ2. Pull-out force of 0.5 kN.

Right frame, File="fd4_b15.dat", Channel 16
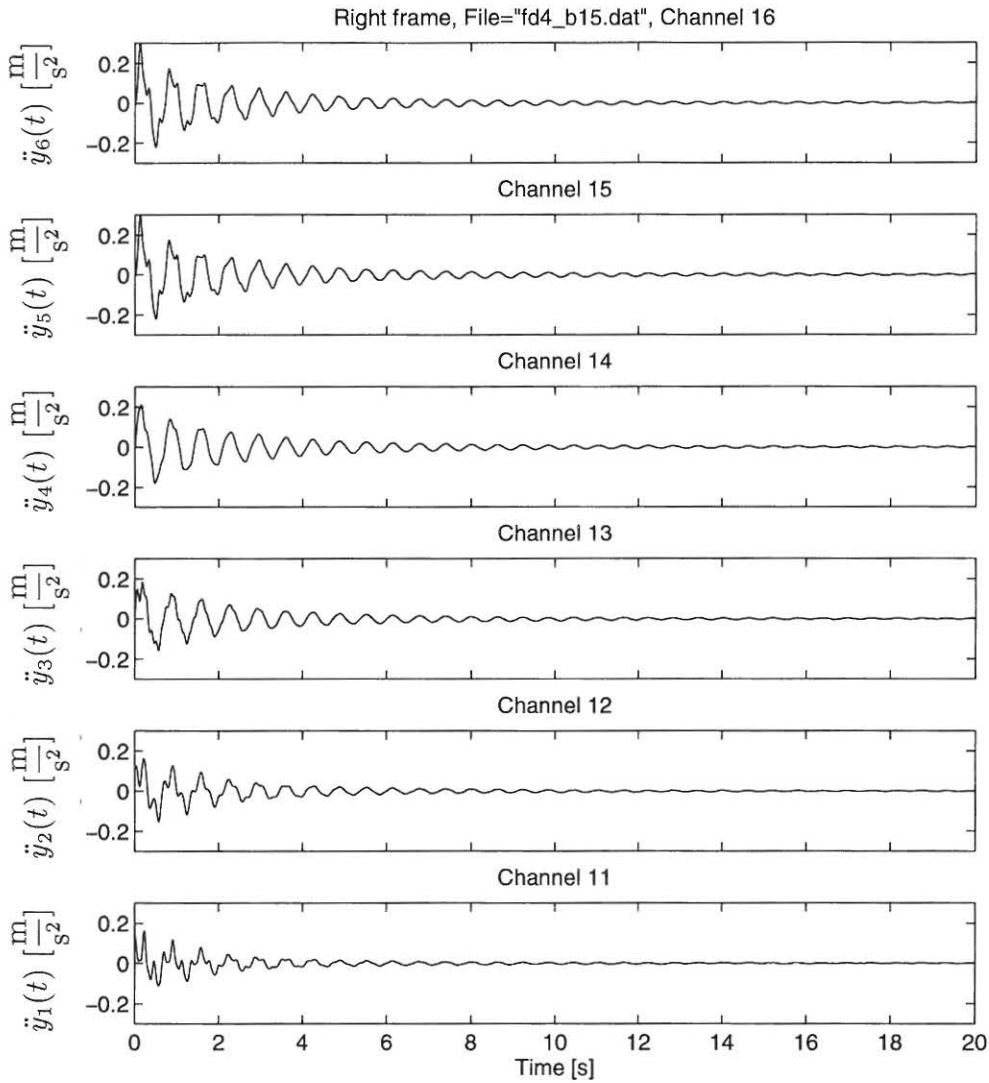
Figure 4.4: Measured accelerations from pull-out test of frame AAUW after EQ3. Pull-out force of 0.5 kN.

The free decay test time series were analyzed using an AutoRegressive Vector model (ARV), Eigen Realization Algorithm (ERA), the Polyreference method (POLYREF) and a AutoRegressiveMoving Average Vector model. The methods produced the modal parameters shown in table1 4.2-4.5.

From tables 4.2-4.5 it is seen that the structure suffer more and more damage as the magnitude of the applied earthquake increases. After the first earthquake a frequency drop of 12% in the first eigenfrequency and and a drop of 13% in the second eigenfrequency are seen. After EQ2 the frequency drop in the first and second mode are 23% and 25%, respectively. After EQ3 the frequency drops are 46% and 48%, respectively.Furthermore, by considering the results from the free decays using varying pull-out forces it is seen that the non-linearity of the structure increases with the degradation of the stiffness.

The damping ratios are seen to increase with the load level in the applied earthquake. After EQ1 the damping ratio of the first mode is increased approximately 120% and approximately 180% in the second mode. After EQ2 the increases are approximately 300% and 400%, respectively. After EQ3 the increases are approximately 400% and 300%, respectively.

Method	State	f_1 [Hz]	f_2 [Hz]	ζ_1 [%]	ζ_2 [%]
ARV	0.25 kN	2.68	8.66	1.12	0.54
ERA	0.25 kN	2.68	8.66	1.14	0.35
POLYREF	0.25 kN	2.67	8.66	1.19	0.70
ARMAV	0.25 kN	2.68	8.66	1.24	0.51
ARV	0.50 kN	2.64	8.58	1.33	0.71
ERA	0.50 kN	2.63	8.58	1.34	0.91
POLYREF	0.50 kN	2.64	8.57	1.44	0.98
ARMAV	0.50 kN	2.64	8.58	1.29	0.68
ARV	0.75 kN	2.62	8.53	1.52	1.13
ERA	0.75 kN	2.61	8.48	1.42	0.95
POLYREF	0.75 kN	2.62	8.50	1.45	0.84
ARMAV	0.75 kN	2.62	8.54	1.53	1.04
ARV	0.25 kN	2.63	8.53	1.27	0.84
ERA	0.25 kN	2.62	8.51	1.32	0.81
POLYREF	0.25 kN	2.63	8.49	1.43	0.89
ARMAV	0.25 kN	2.63	8.52	1.39	0.83

Table 4.2: *Estimated modal parameters for virgin frame AAUW.*

Method	State	f_1 [Hz]	f_2 [Hz]	ζ_1 [%]	ζ_2 [%]
ARV	0.25 kN	2.31	7.46	2.28	1.52
ERA	0.25 kN	2.30	7.46	2.05	1.36
POLYREF	0.25 kN	2.31	7.47	1.81	1.33
ARMAV	0.25 kN	2.33	7.46	2.44	1.55
ARV	0.50 kN	2.22	7.18	2.93	2.01
ERA	0.50 kN	2.21	7.19	2.94	1.73
POLYREF	0.50 kN	2.23	7.20	2.94	1.80
ARMAV	0.50 kN	2.23	7.18	2.87	2.06
ARV	0.75 kN	2.16	7.01	3.27	2.06
ERA	0.75 kN	2.15	7.02	3.11	1.86
POLYREF	0.75 kN	2.17	7.03	3.27	1.81
ARMAV	0.75 kN	2.16	7.00	3.21	2.04
ARV	0.50 kN	2.24	7.26	2.99	1.87
ERA	0.50 kN	2.23	7.25	2.98	1.63
POLYREF	0.50 kN	2.25	7.27	2.81	1.64
ARMAV	0.50 kN	2.25	7.26	2.28	1.96

Table 4.3: *Estimated modal parameters of frame AAUW after EQ1.*

Method	State	f_1 [Hz]	f_2 [Hz]	ζ_1 [%]	ζ_2 [%]
ARV	0.25 kN	1.88	5.90	2.97	2.39
ERA	0.25 kN	1.87	5.92	3.16	2.63
POLYREF	0.25 kN	1.90	5.91	2.80	2.70
ARMAV	0.25 kN	1.89	5.91	3.60	2.77
ARV	0.50 kN	1.78	5.59	3.58	3.20
ERA	0.50 kN	1.78	5.60	4.13	3.61
POLYREF	0.50 kN	1.80	5.58	3.96	4.03
ARMAV	0.50 kN	1.78	5.59	3.73	3.67
ARV	0.75 kN	1.72	5.48	4.67	4.72
ERA	0.75 kN	1.71	5.40	4.44	3.93
POLYREF	0.75 kN	1.73	5.37	4.31	4.45
ARMAV	0.75 kN	1.73	5.47	4.93	4.81
ARV	0.50 kN	1.81	5.69	4.01	3.87
ERA	0.50 kN	1.80	5.69	4.07	3.79
POLYREF	0.50 kN	1.83	5.65	3.94	3.71
ARMAV	0.50 kN	1.82	5.70	4.69	4.11

Table 4.4: *Estimated modal parameters of frame AAUW after EQ2.*

Method	State	f_1 [Hz]	f_2 [Hz]	ζ_1 [%]	ζ_2 [%]
ARV	0.25 kN	1.54	4.84	3.57	2.28
ERA	0.25 kN	1.53	4.82	3.07	2.34
POLYREF	0.25 kN	1.55	4.82	3.34	2.20
ARMAV	0.25 kN	1.57	4.84	4.09	2.27
ARV	0.50 kN	1.42	4.50	4.80	3.56
ERA	0.50 kN	1.42	4.49	6.02	2.63
POLYREF	0.50 kN	1.43	4.50	4.46	2.71
ARMAV	0.50 kN	1.43	4.49	5.14	3.34
ARV	0.75 kN	1.38	4.36	4.37	3.54
ERA	0.75 kN	1.37	4.36	4.55	3.20
POLYREF	0.75 kN	1.38	4.36	4.43	2.90
ARMAV	0.75 kN	1.38	4.34	4.73	3.57

Table 4.5: *Estimated modal parameters of frame AAUW after EQ3.*

Using the the four presented methods it is possible to obtain estimates of the modeshapes as well. The results of the mode shape identification of the virgin structure are shown in figures 4.5-4.7 for the three load cases 0.25 kN, 0.50 kN and 0.75 kN.
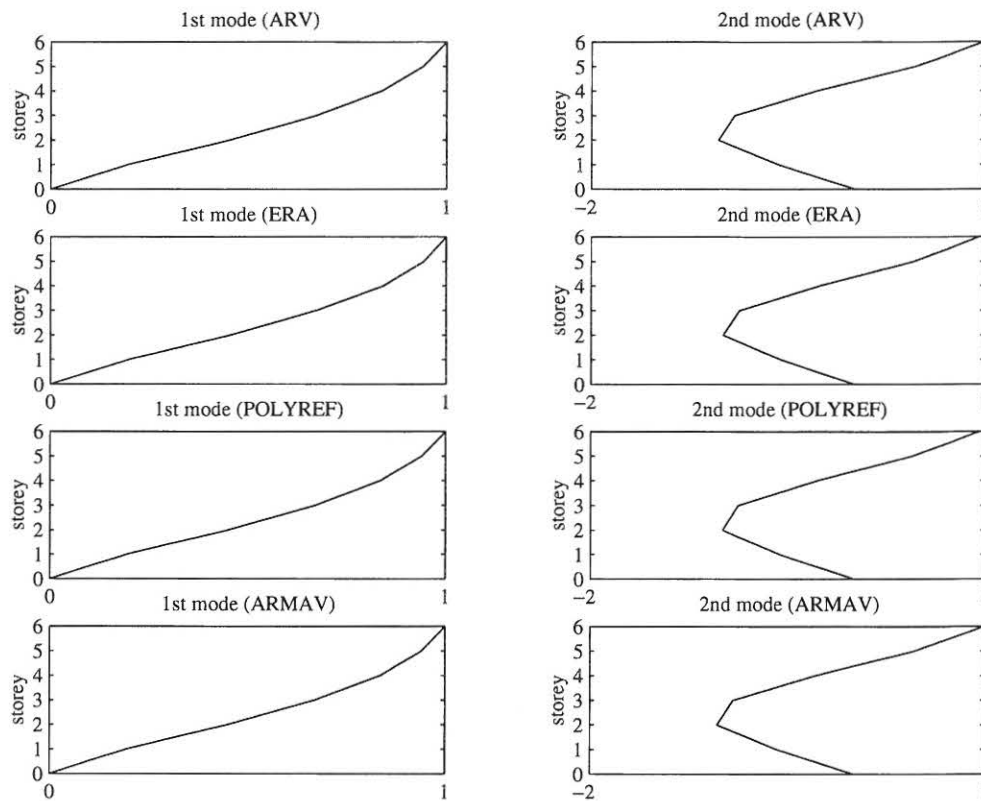

Figure 4.5: Estimated mode shapes of frame AAUW in the virgin state. Pull-out force 0.25 kN.
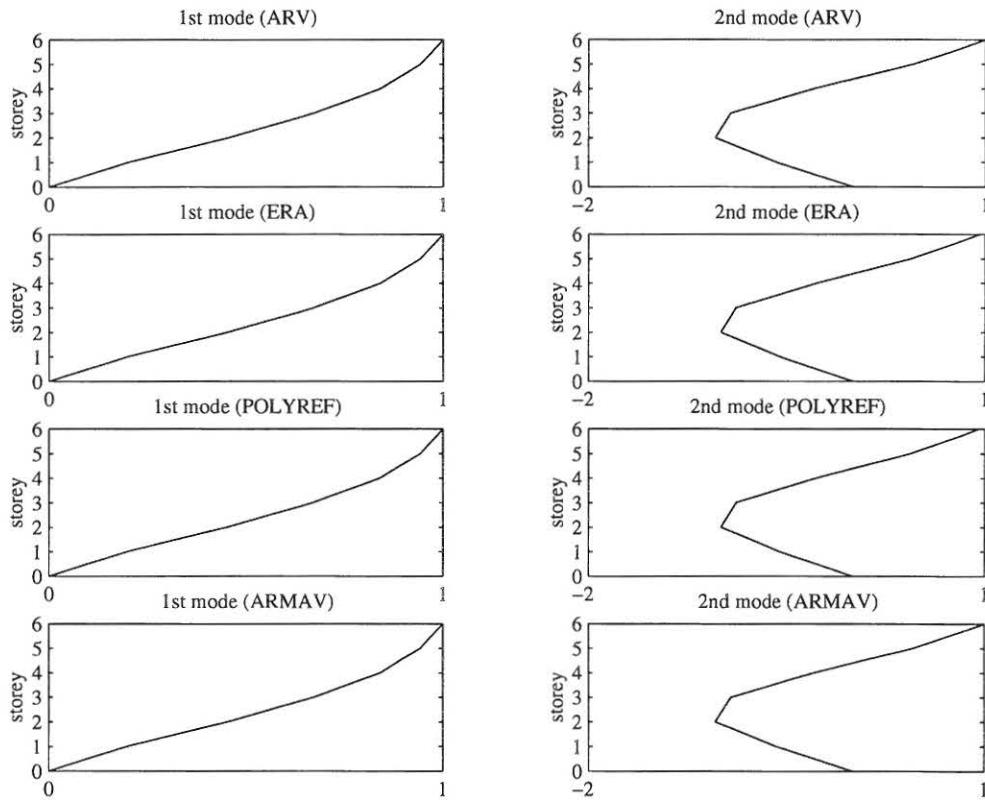
Figure 4.6: Estimated mode shapes of frame AAUW in the virgin state. Pull-out force 0.50 kN.
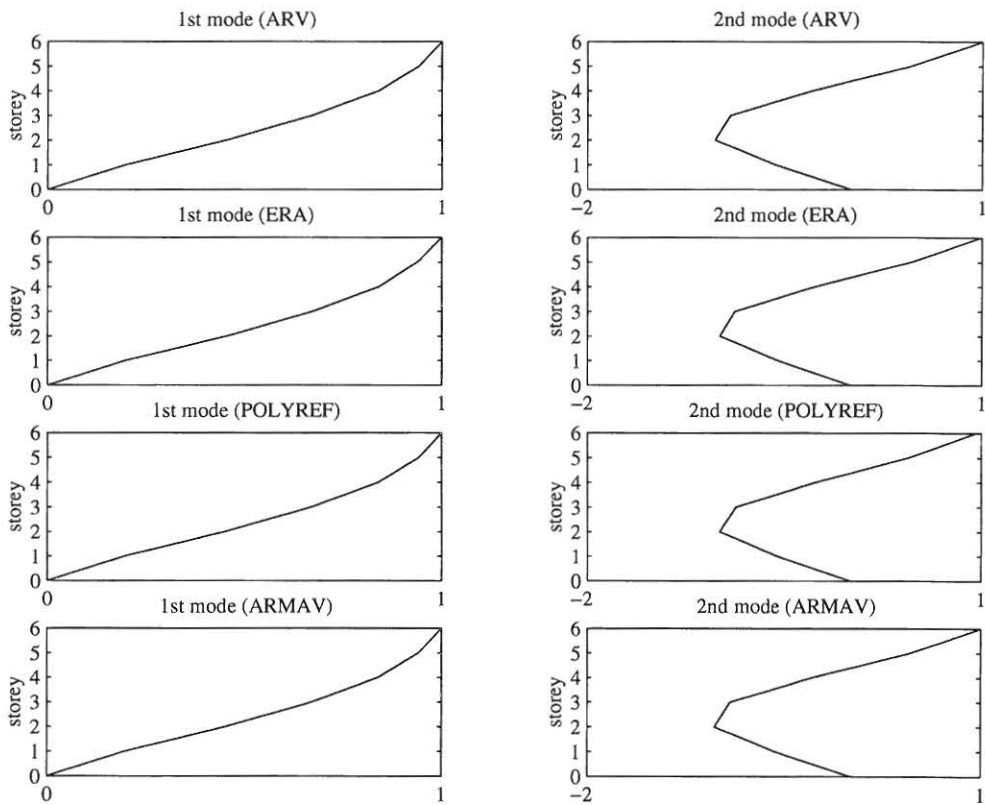

Figure 4.7: Estimated mode shapes of frame AAUW in the virgin state. Pull-out force 0.75 kN.

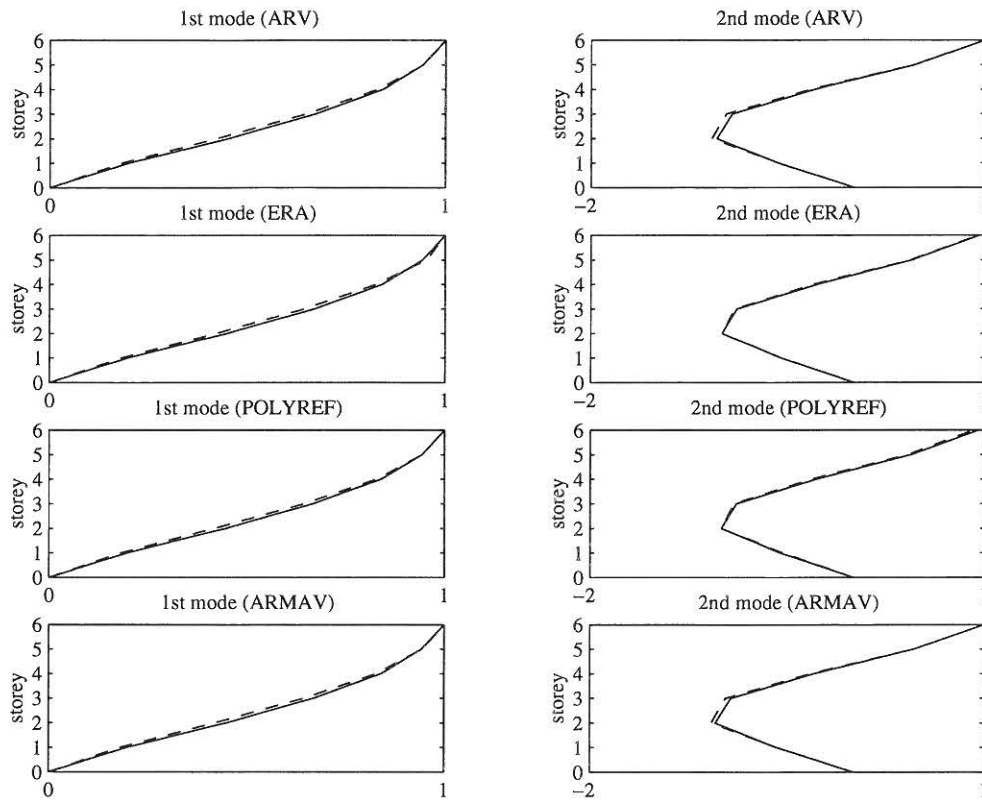In figures 4.8-4.10 the corresponding modeshapes after EQ1 are shown.

Figure 4.8: Estimated mode shapes of frame AAUW after EQ1. Pull-out force 0.25 kN. [———]: Virgin structure. [− − −]: Damaged structure.

Figure 4.9: Estimated mode shapes of frame AAUW after EQ1. Pull-out force 0.50 kN. [——]: Virgin structure. [– – –]: Damaged structure.

Figure 4.10: Estimated mode shapes of frame AAUW after EQ1. Pull-out force 0.75 kN. [——]: Virgin structure. [– – –]: Damaged structure.

In figures 4.11-4.13 the corresponding modeshapes after EQ2 are shown.

Figure 4.11: Estimated mode shapes of frame AAUW after EQ2. Pull-out force 0.25 kN. [——]: Virgin structure. [– – –]: Damaged structure.
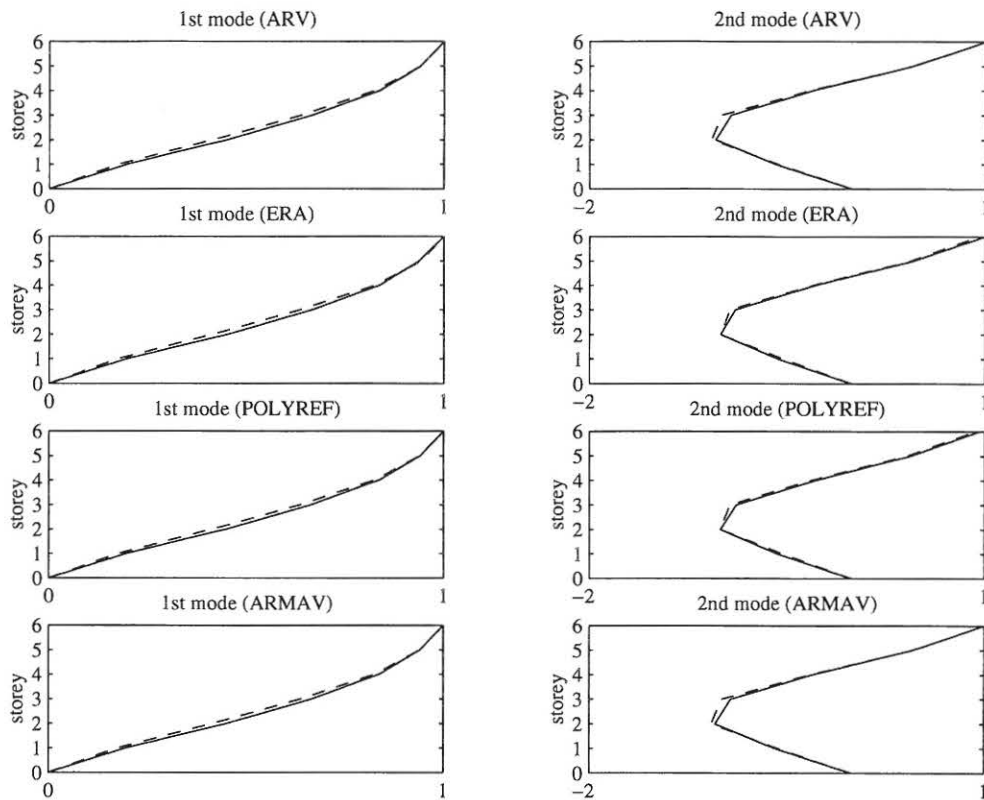
Figure 4.12: Estimated mode shapes of frame AAUW after EQ2. Pull-out force 0.50 kN. [——]: Virgin structure. [− − −]: Damaged structure.
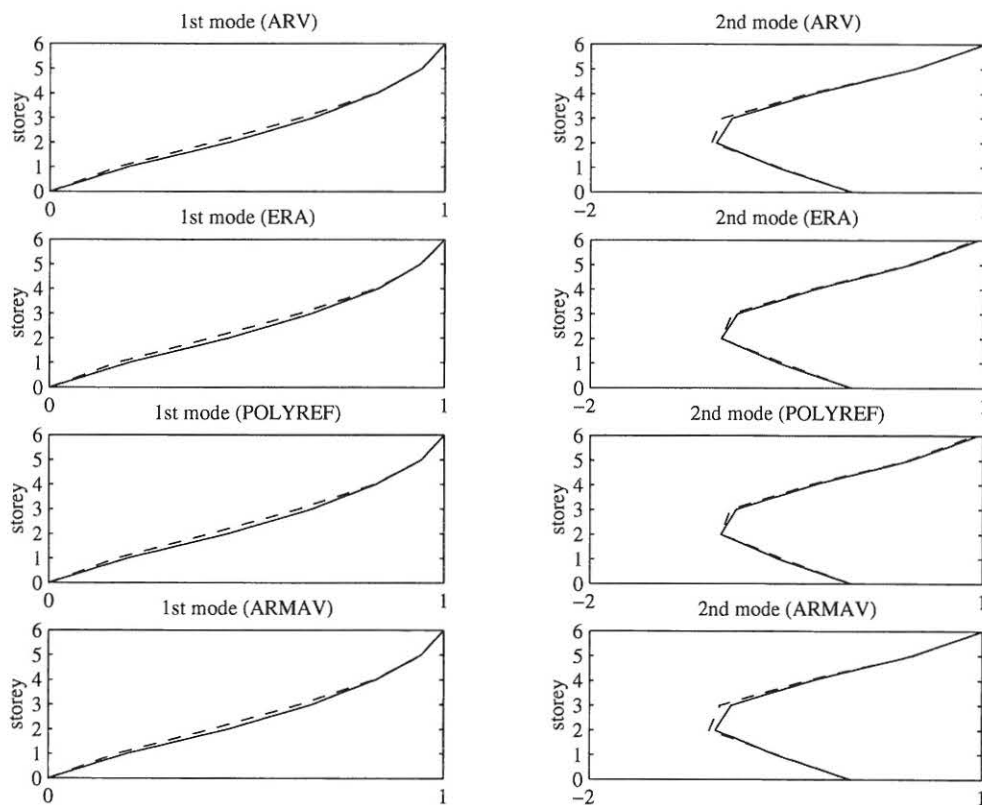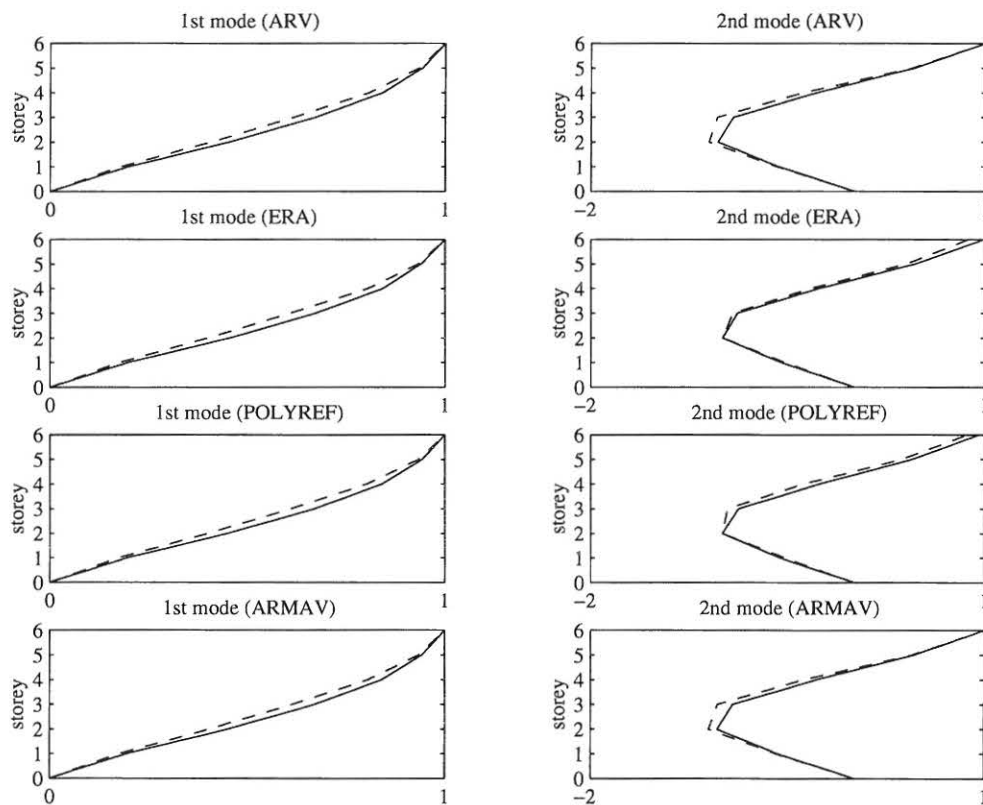

Figure 4.13: Estimated mode shapes of frame AAUW after EQ2. Pull-out force 0.75 kN. [——]: Virgin structure. [− − −]: Damaged structure.

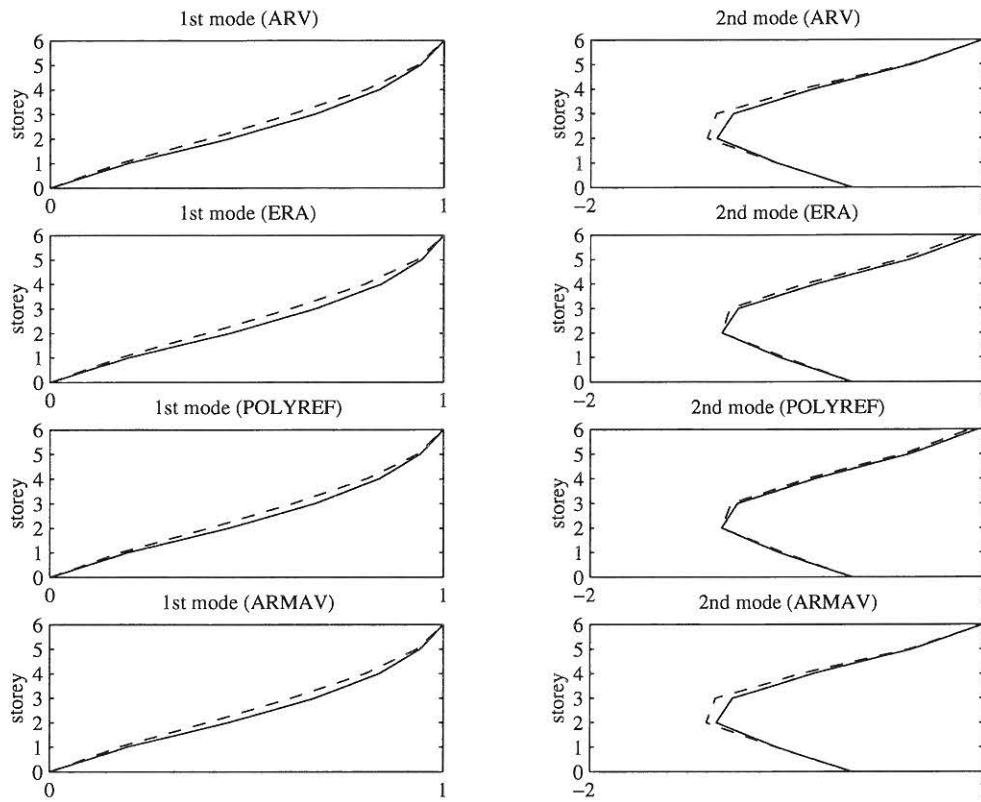In figures 4.14-4.16 the corresponding modeshapes after EQ3 are shown.
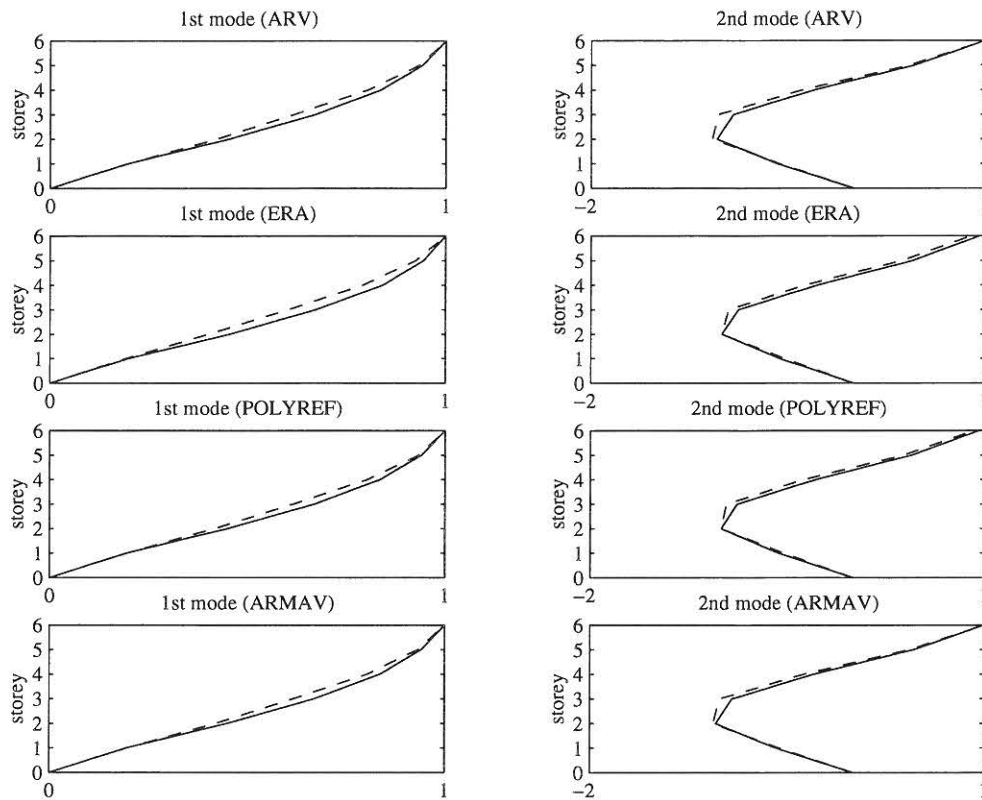
Figure 4.14: Estimated mode shapes of frame AAUW after EQ3. Pull-out force 0.25 kN. [——]: Virgin structure. [− − −]: Damaged structure.

From figures 4.6-4.16 is concluded that generally only small changes in the mode shapes occurs during the damage process. Hence these seems of little use for application in damage localization and quantification procedures.
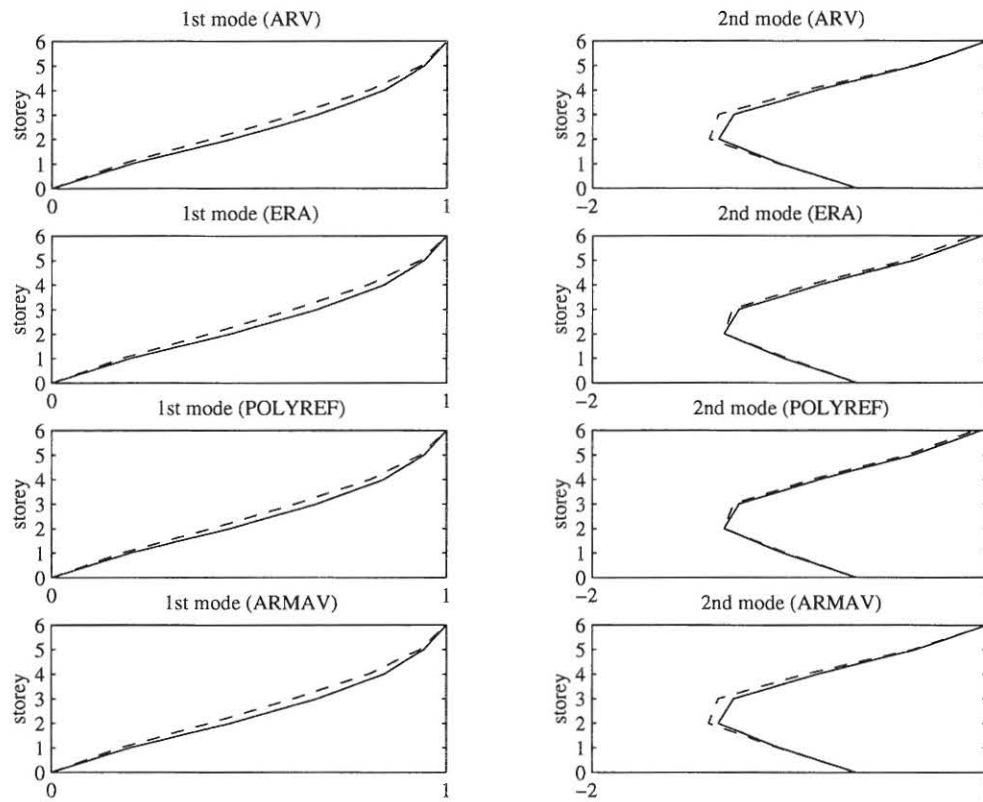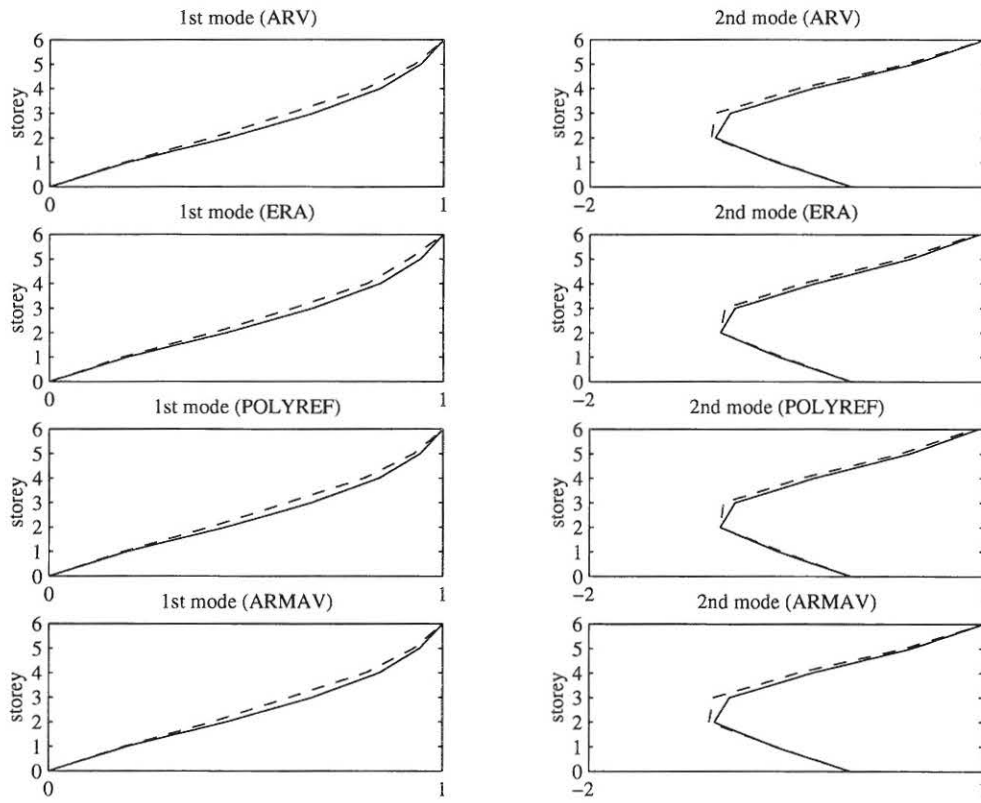
Figure 4.15: Estimated mode shapes of frame AAUW after EQ3. Pull-out force 0.50 kN. [——]: Virgin structure. [− − −]: Damaged structure.
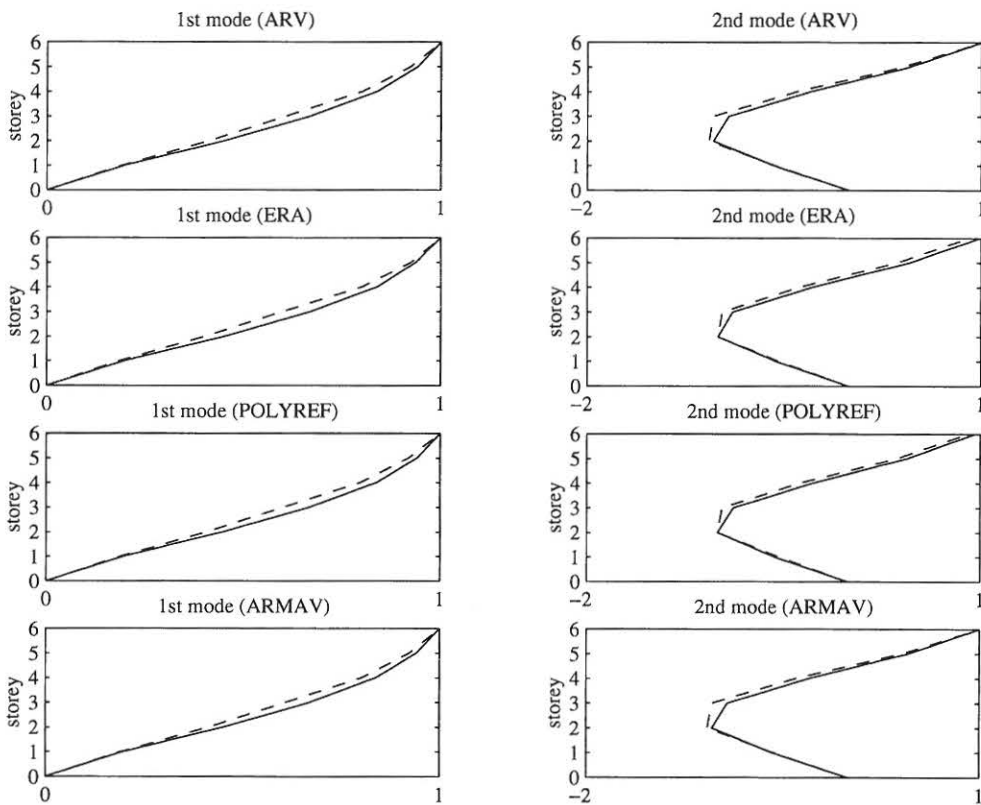
Figure 4.16: Estimated mode shapes of frame AAUW after EQ3. Pull-out force 0.75 kN. [——]: Virgin structure. [− − −]: Damaged structure.

Chapter 5

Destructive testing

In this chapter data sampled during and after strong motions are presented. In the destructive testing the frame AAUW is exposed to three sequential earthquakes of increasing magnitude called EQ1, EQ2 and EQ3. These are shown in figure 5.1.
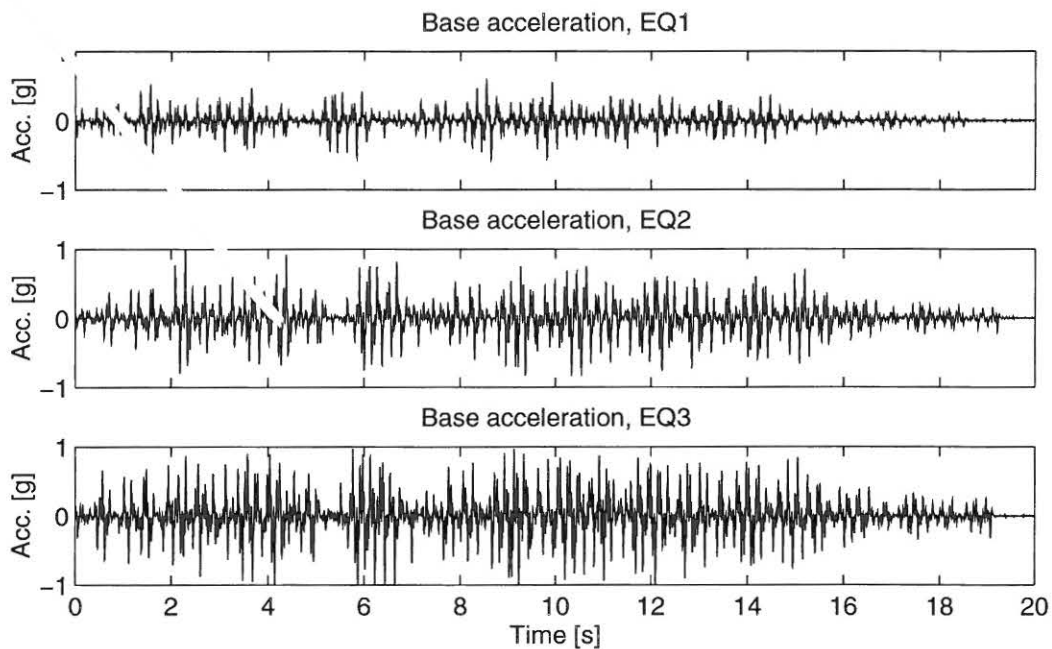
Figure 5.1: The three applied earthquakes in units of g.

The time series shown in figure 5.1 were generated by filtering white noise through a Kanai-Tajimi filter with a circular frequency of 4.8 Hz and a damping ratio of 0.1. With structural modes at 2.64 Hz and 8.58 Hz the dominant frequencies in the load process are placed in between the two lowest modes of the structure.

The files with the data from the strong motion testing are named as shown in table 5.1.

Name	Case
sm4_20b.dat	Strong motion earthquake EQ1 with a peak acceleration of 0.36g
sm4_40b.dat	Strong motion earthquake EQ2 with a peak acceleration of 0.73g
sm4_55b.dat	Strong motion earthquake EQ3 with a peak acceleration of 1g

Table 5.1: *File names for the data from destructive testing. Frame AAUW.*

5.1   Results for frame AAUW

In this section the raw as well as the processed data obtained from the strong motion records during the three runs shown in figure 5.1 are presented. In figures 5.2, 5.4 and 5.6 the acceleration records measured at the storeys during the three runs are shown. It can be seen that the maximum top-storey acceleration during EQ1 is 4.3 $\frac{m}{s^2}$, during EQ2 is 15 $\frac{m}{s^2}$ and during EQ3 is 19 $\frac{m}{s^2}$.

In figures 5.3, 5.5 and 5.7 the applied cylinder force and displacements are shown during the three runs, respectively.

Figure 5.2: Measured accelerations during EQ1 for frame AAUW.

Figure 5.3: Measured shaking table displacement and cylinder force during EQ1 for frame AAUW.
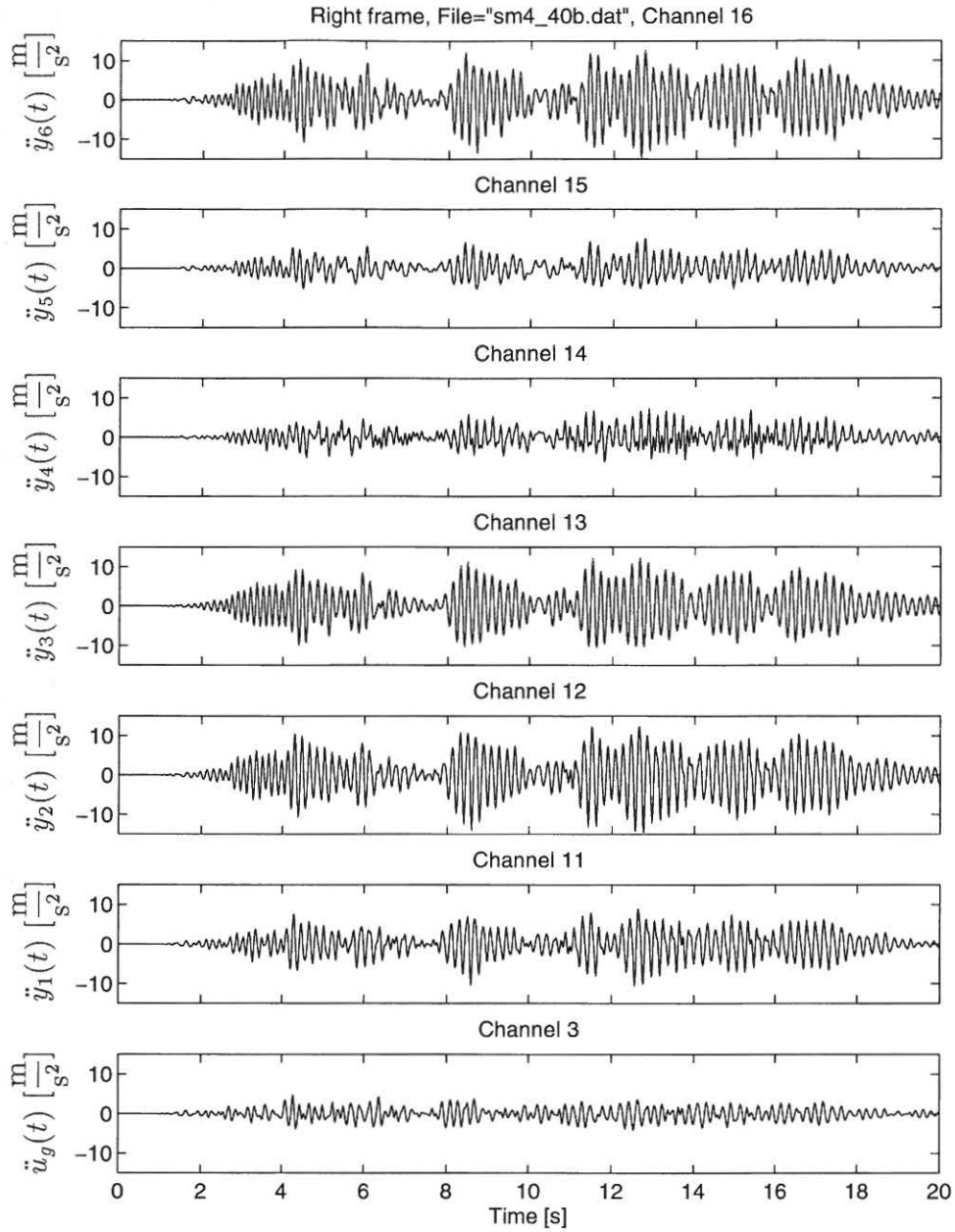
Figure 5.4: Measured accelerations during EQ2 for frame AAUW.
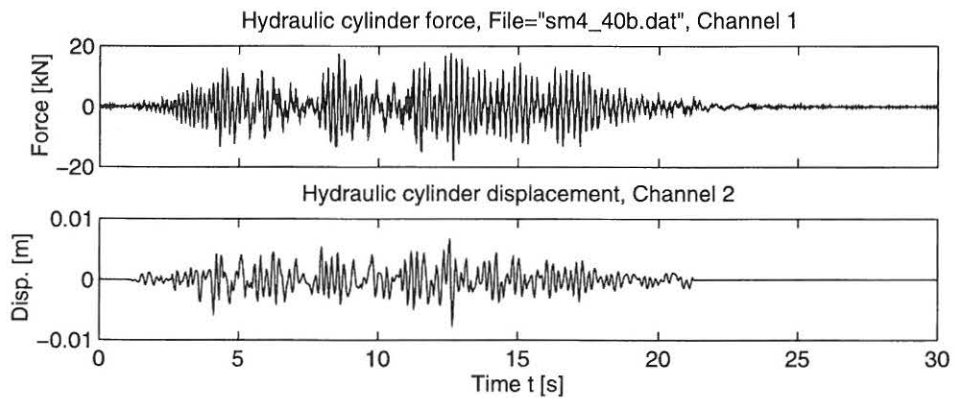
Figure 5.5: Measured shaking table displacement and cylinder force during EQ2 for frame AAUW.

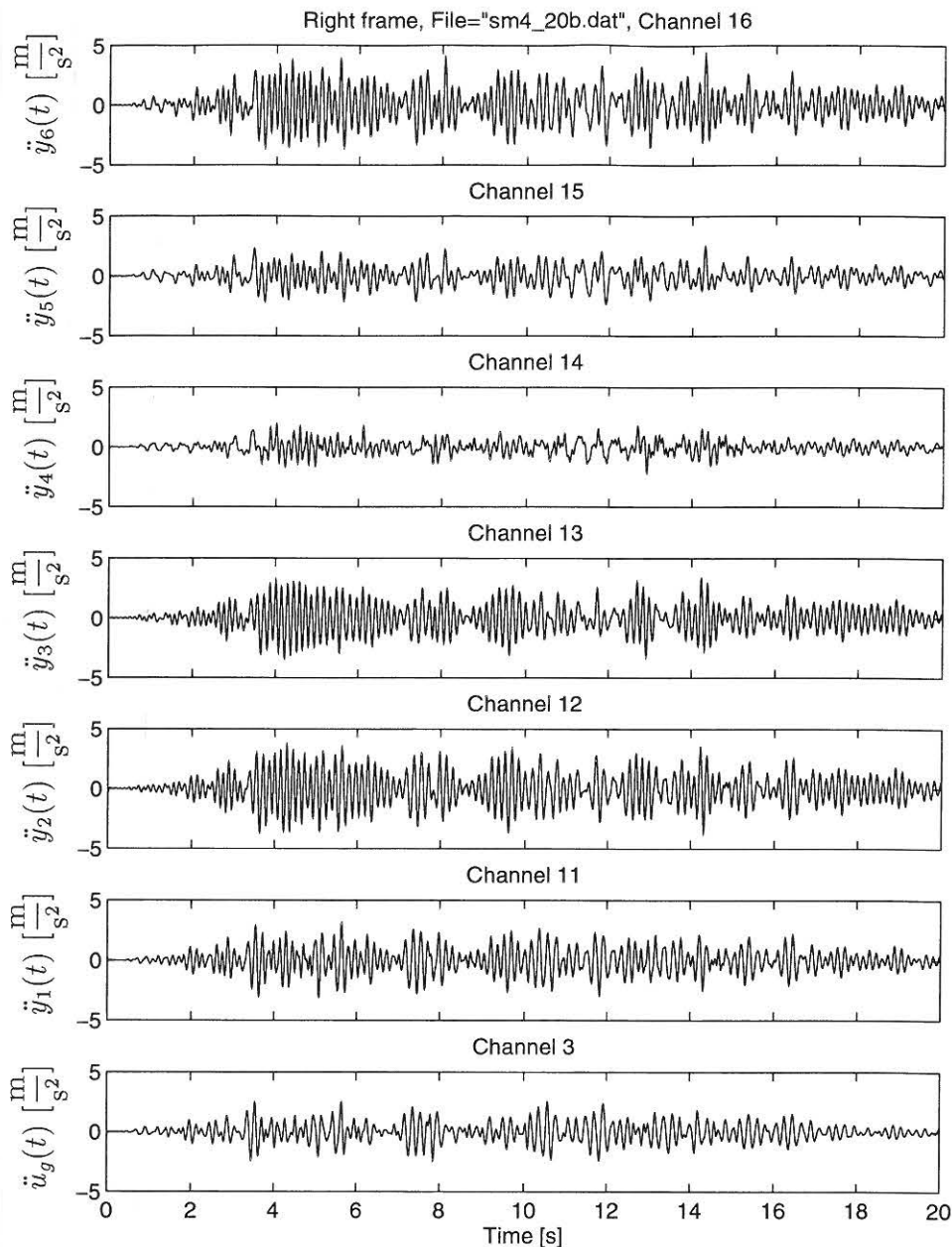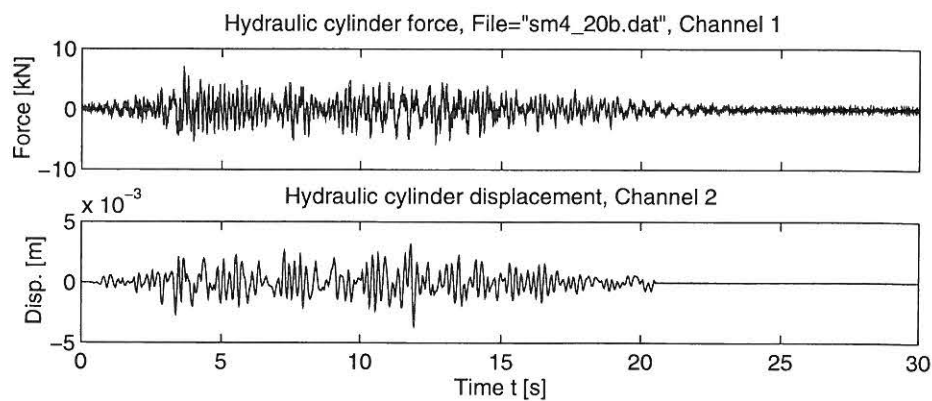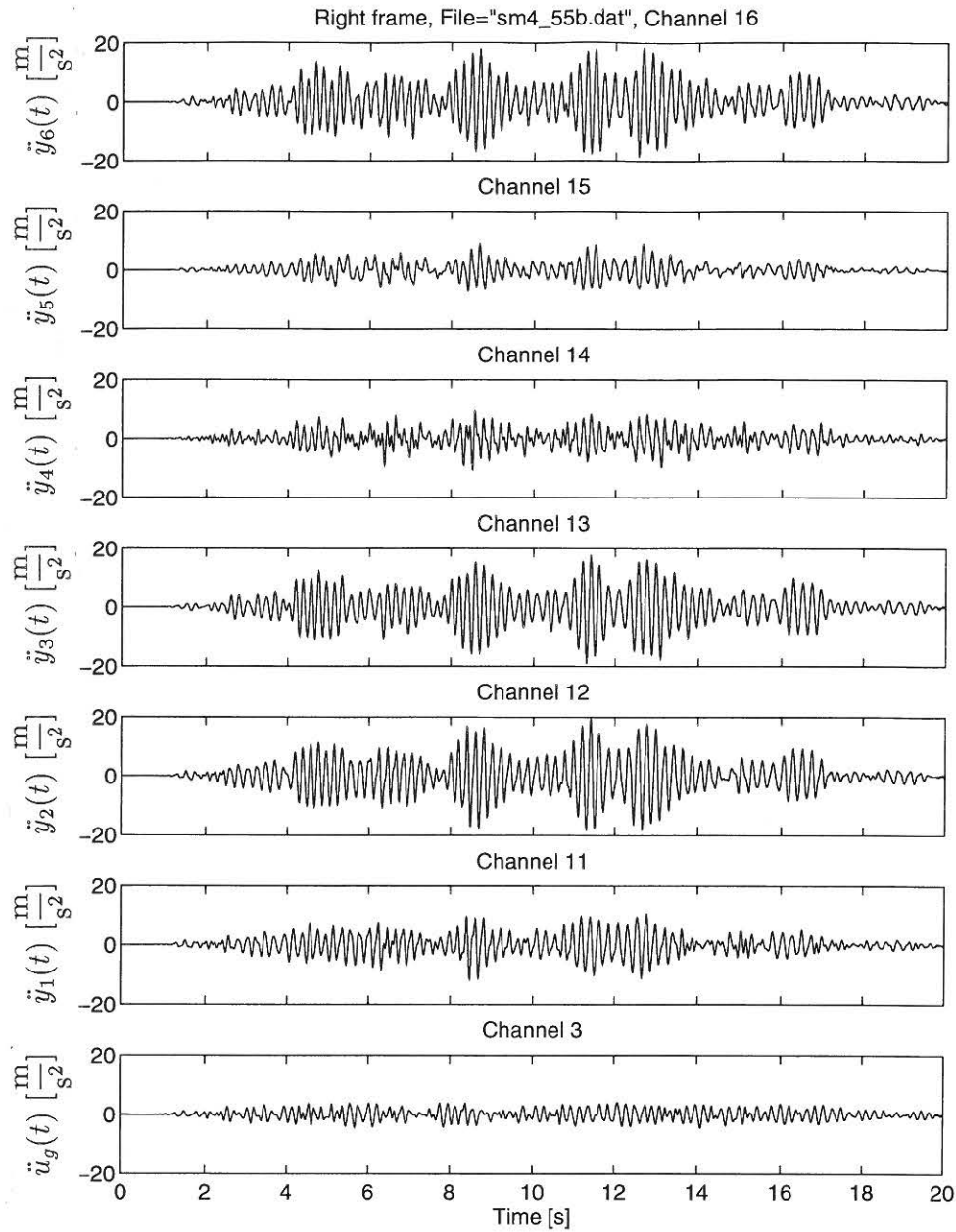Figure 5.6: Measured accelerations during EQ3 for frame AAUW.
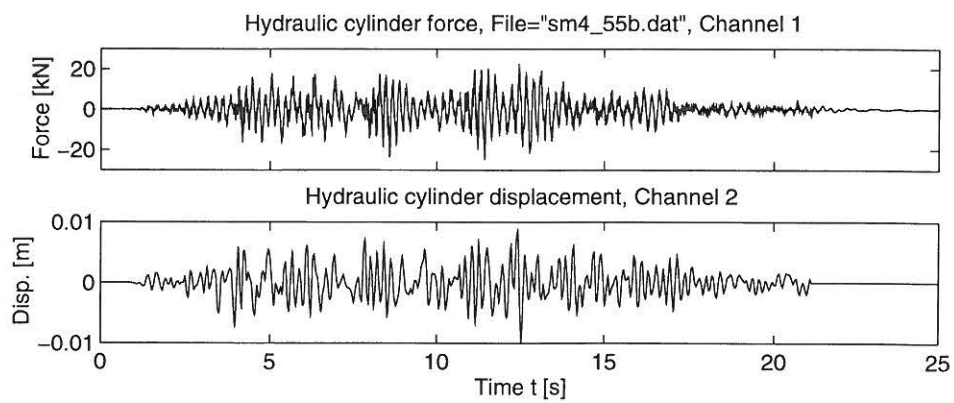
Figure 5.7: Measured shaking table displacement and cylinder force during EQ3 for frame AAUW.

5.1.1 Processed data

This section presents processed data where inter-storey and top-storey displacements have been found using double time integration procedures as described in e.g. Skjærbæk [40]. Furthermore, time series of eigenfrequencies are extracted from the strong motion records. The procedure for frequency estimation is described in Kirkegaard et al. [15].
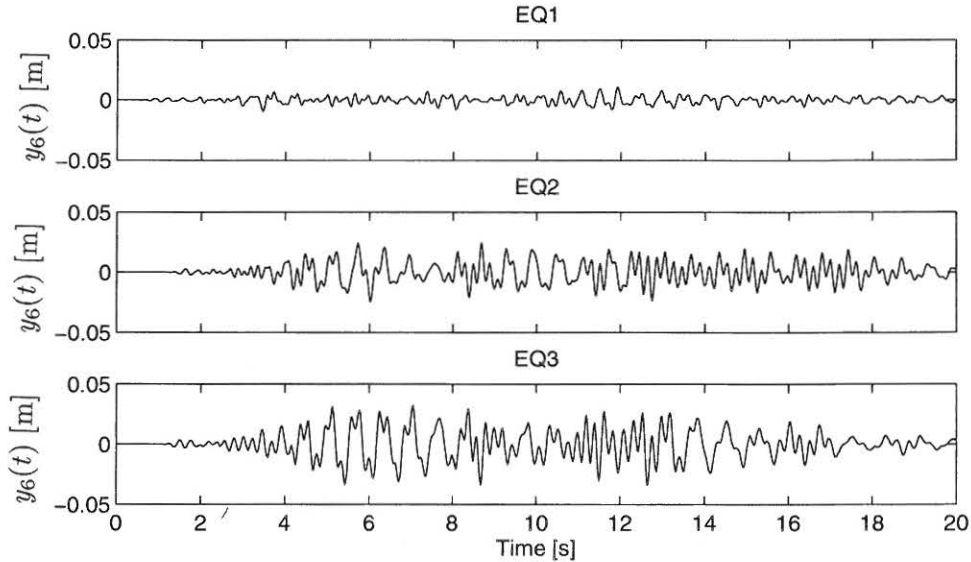
Figure 5.8: Top storey displacements during EQ1, EQ2 and EQ3.

In figures 5.9-5.11 the interstorey displacements during the three earthquakes are shown, respectively.

From figure 5.9 the maximum interstorey drift is seen to be approximately 2.7 mm in the weak fourth storey during EQ1. During EQ2 the maximum interstorey drift in storey 5 is 10 mm and during EQ3 it is 18 mm in storey 5.

During the integration process where displacements are obtained a Butterworth 6th order high-pass digital filter with a cut-off frequency of 0.95 Hz and a Butterworth 8th order low-pass digital filter with a cut-off frequency of 20 Hz have been used.
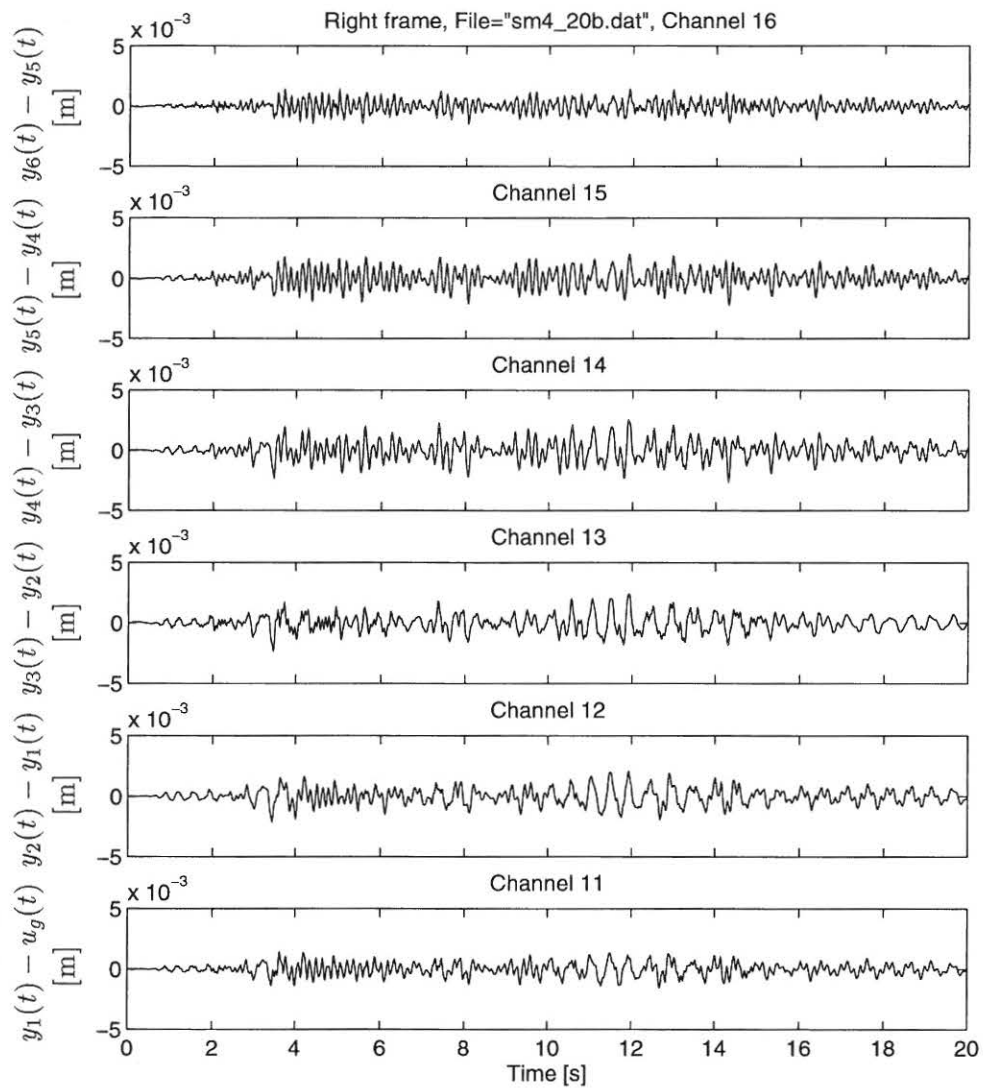
Figure 5.9: Interstorey displacements during EQ1 for frame AAUW.
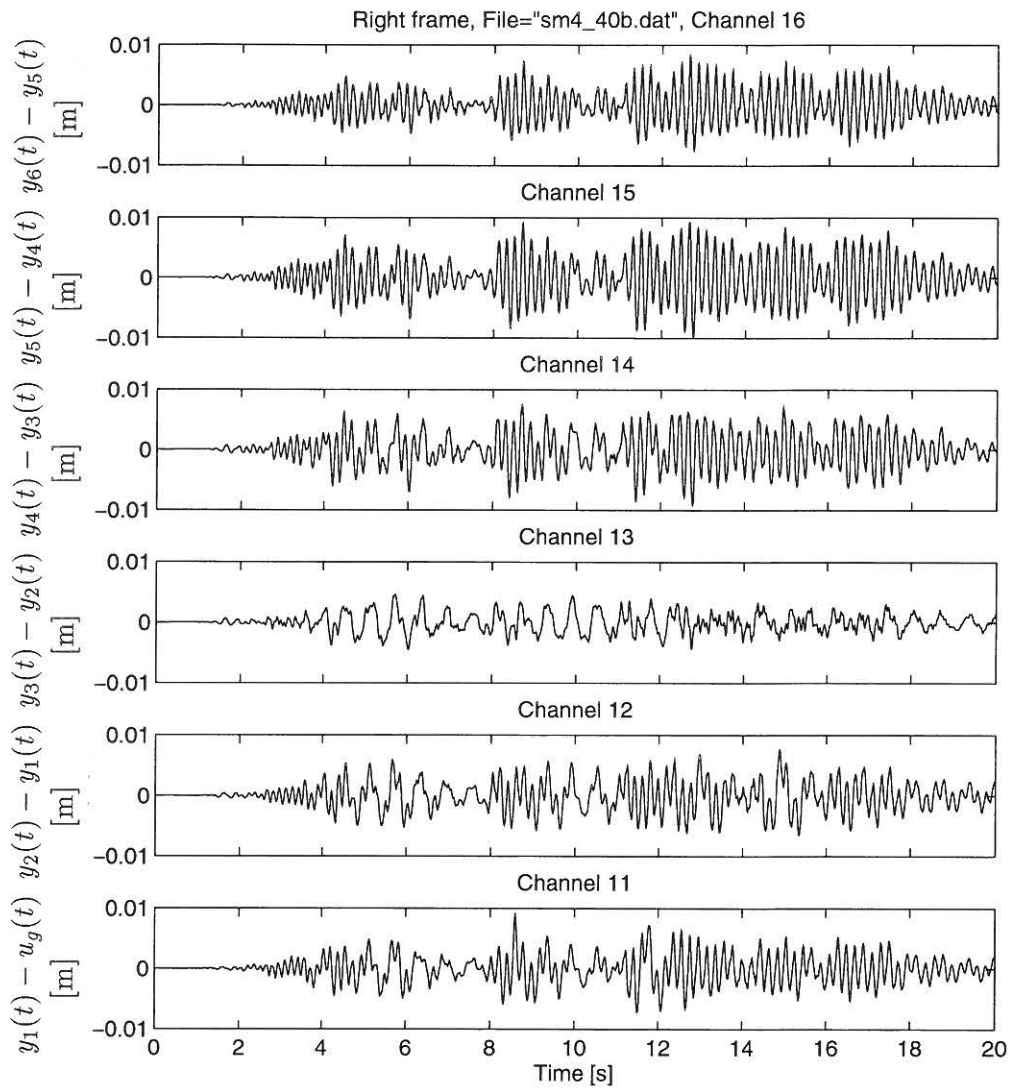
Figure 5.10: Interstorey displacements during EQ2 for frame AAUW.
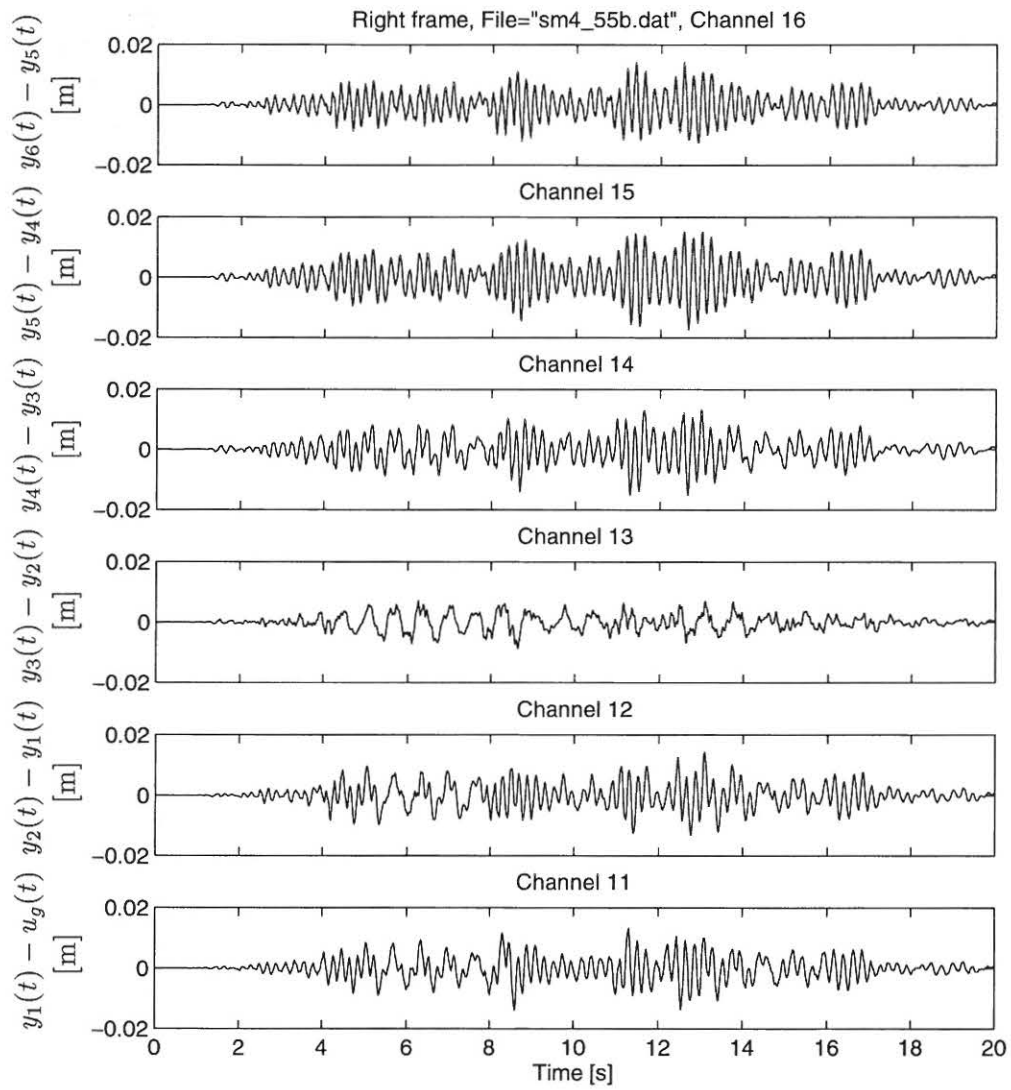
Figure 5.11: Interstorey displacements during EQ3 for frame AAUW.

In order to evaluate the development of the natural frequencies of the structure during the earthquakes a recursive implemented ARMAV model have been fitted to the measured acceleration time series, see Kirkegaard et al. [15]. The evaluated development in the two lowest eigenfrequencies are shown in figures 5.12-5.14 for the three earthquakes, respectively.
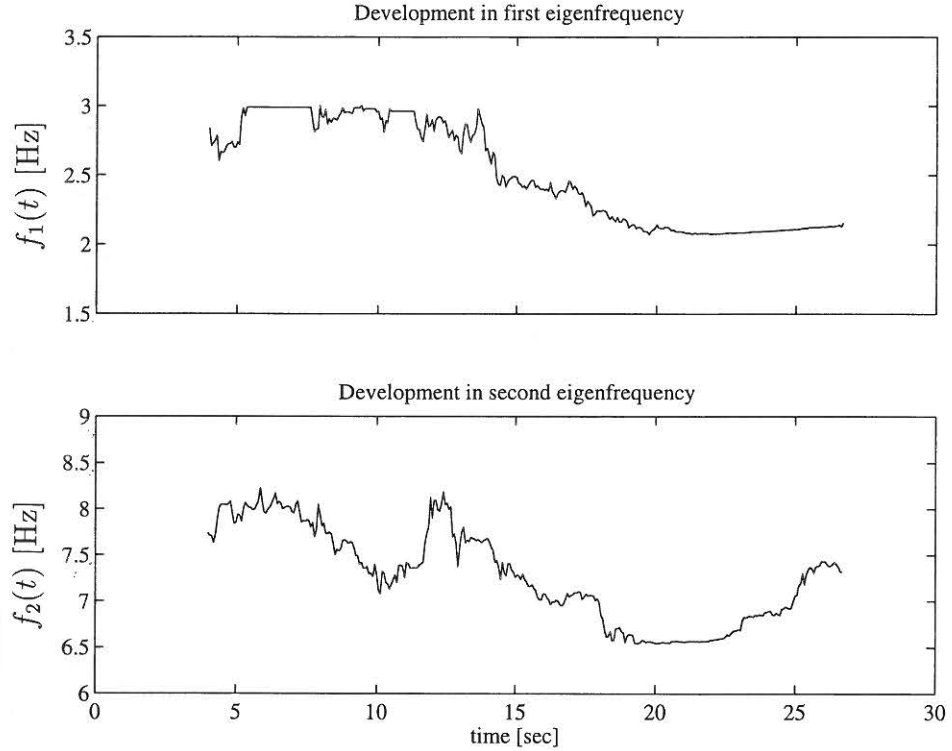
Figure 5.12: Development of eigenfrequencies in first and second mode during EQ1.

For each of the eigenfrequency time series the maximum softening is evaluated for the two lowest eigenfrequencies.

Generally the multi-dimensional maximum softening $\delta_{M,i}$ is defined according to Nielsen et al. [23], [24] as

$$\delta_{M,i} = 1 - \frac{T_{i,0}}{T_{i,\max}} \tag{5.1}$$

Where $T_{i,0}$ is the initial value of the ith eigenperiod for the undamaged structure and $T_{i,\max}$ is the maximum value of the ith eigenperiod during the earthquake.

The maximum softenings during the three runs are shown in table 5.2.

	$f_{\min,1}$ [Hz]	$f_{\min,2}$ [Hz]	$\delta_{M,1}$	$\delta_{M,2}$
EQ1	2.07	6.54	0.22	0.24
EQ2	1.57	5.15	0.41	0.40
EQ3	1.31	4.49	0.50	0.48

Table 5.2: *Estimated minimum frequencies and maximum softenings during the three earthquakes.*
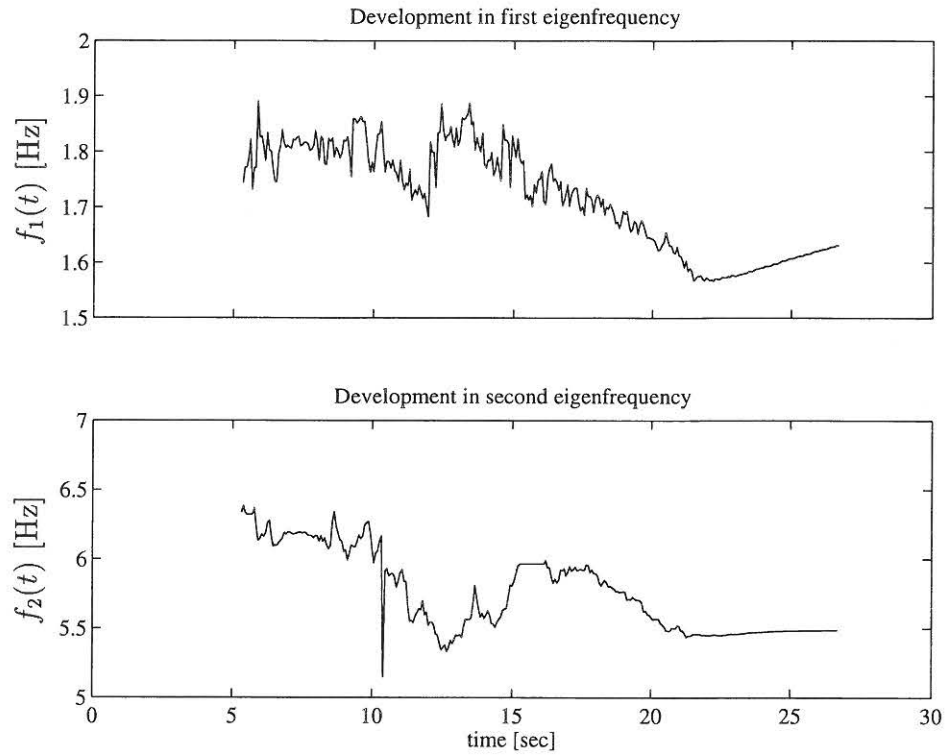
Figure 5.13: Development of eigenfrequencies in first and second mode during EQ2.
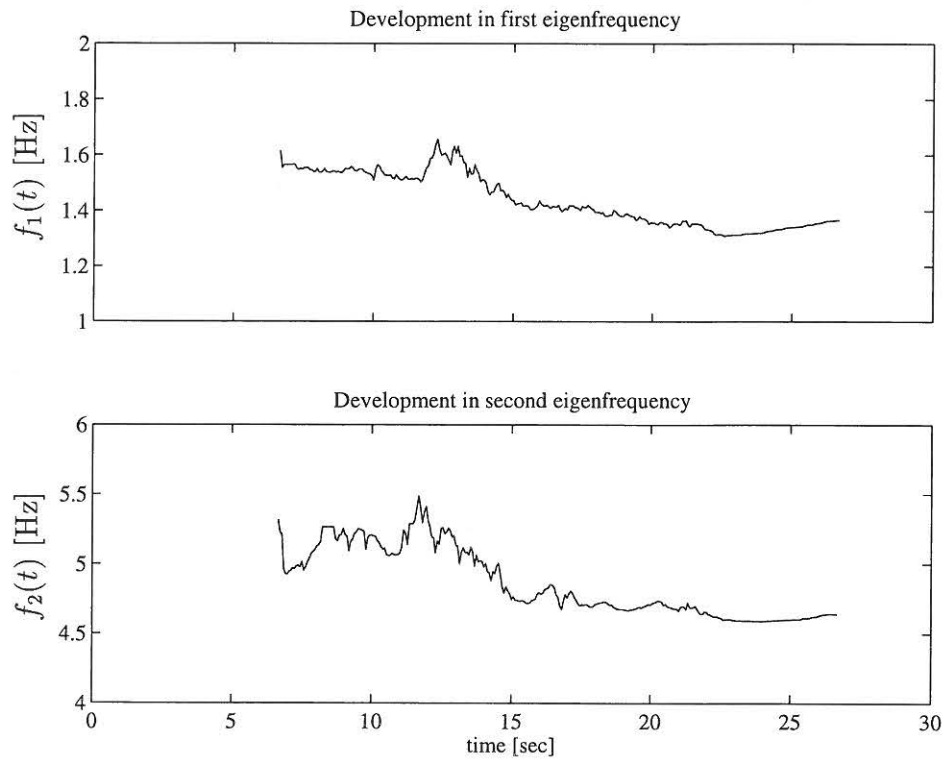
Figure 5.14: Development of eigenfrequencies in first and second mode during EQ3.

Chapter 6

Static tests

In order to evaluate the damage state of the structure, the structure is exposed to static tests after each earthquake event. Two types of tests are used:

1. Static tests with the entire structure.

2. Static tests with individual beams and columns.

6.1 Static testing of entire structure

In the static tests with the entire structure a definite force is applied at the top storey and displacements are measured at each of the storey. The force is varied between 0 and 0.75 kN. A Schematical view of the test set-up is shown in figure 6.1.
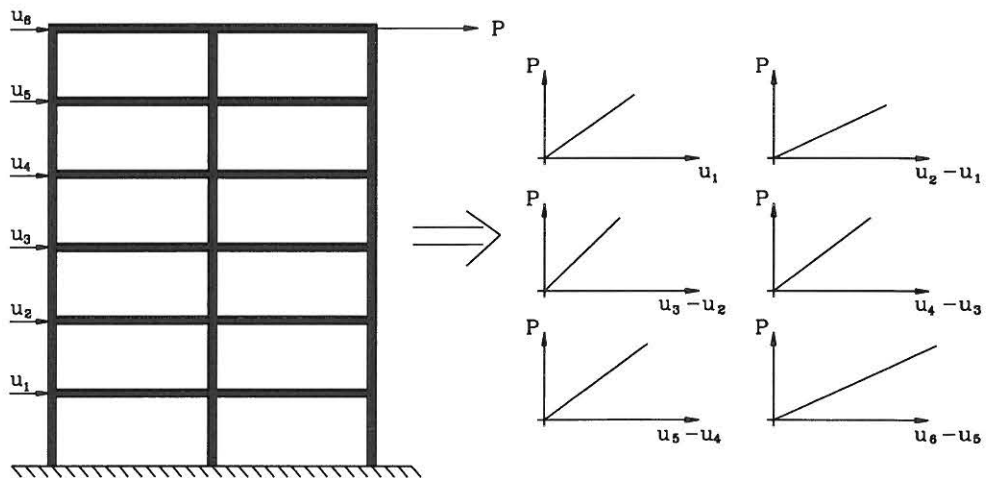
Figure 6.1: Schematic test set-up used for the static test with the entire structure and the relative displacement versus force diagrams.

6.1.1   Results

The static testing was performed on the entire structure in the virgin state and after each of the three strong motion events.

In figure 6.2 the results of the static tests are shown.
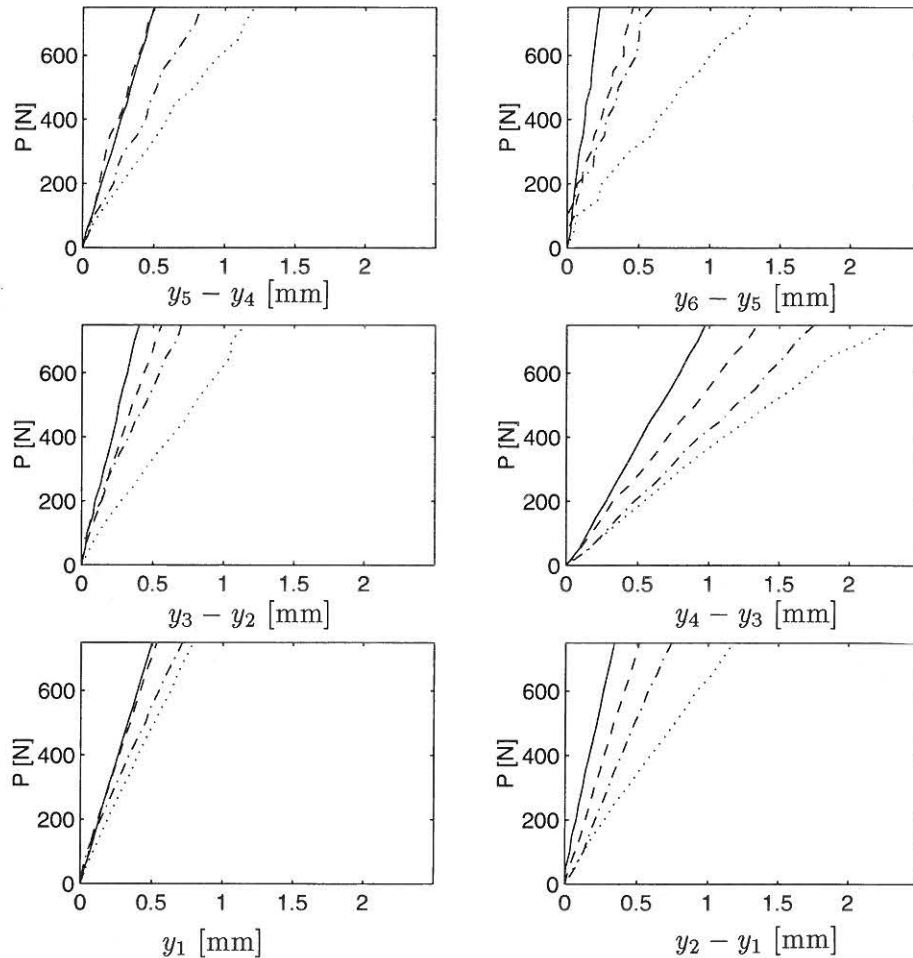
Figure 6.2: Force-deformation curves obtained from the static testings of the frame. [———]: Virgin structure, $[---]$: After EQ1, $[-. - .-]$: After EQ2 and [...]: After EQ3.

As it can be seen from figure 6.2 the relative displacement of the 4th storey is about 2.5 times higher than the average of the rest of the storeys in the virgin state, 2.7 times higher after EQ1, 2.5 times higher after EQ2. As expected the deformations increase a lot after EQ3. It should be noted that a soft behaviour is also present in the top storey after EQ3, but still the relative displacement of the 4th storey is about 2.2 times higher than the average displacement value of the rest of the storeys.

In figure 6.3 the total deformations at maximum load are shown.
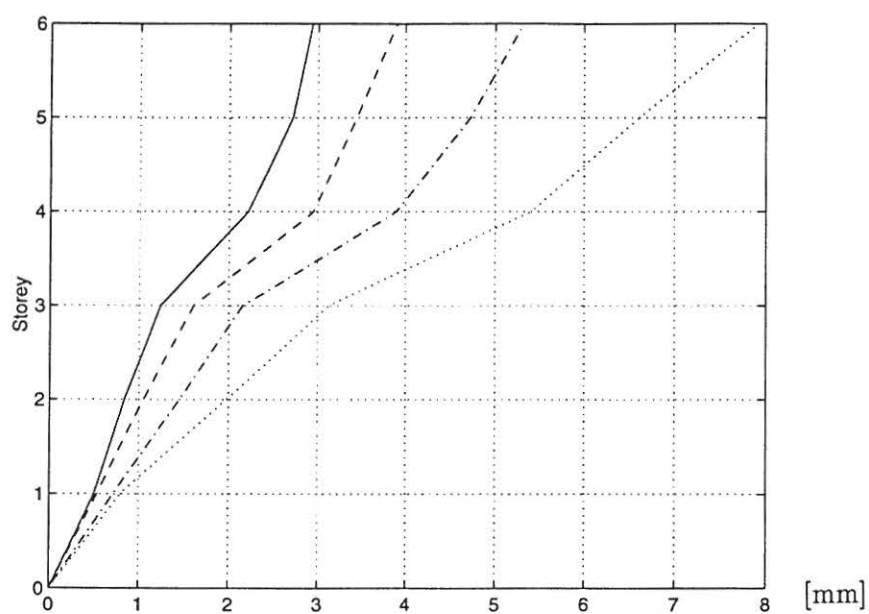
Figure 6.3: Total deformations at maximum load. [———]: Virgin structure, [– – –]: After EQ1, [–. – .–]: After EQ2 and [...]: After EQ3.

6.2   Static testing of beams and columns

After the last dynamic test the structure is cut into pieces and each of the beams and columns are subjected to static tests where corresponding force and deformation are measured. The columns are loaded laterally within the range of 0 to 1.5 kN and the beams are loaded within the range of 0 to 0.4 kN.

6.2.1   "Cut up" of test frame

In order to avoid the introduction of damage during the cutting of the frames a highspeed diamantbased cutting device was used. The "cut up" is illustrated in figure 6.4.
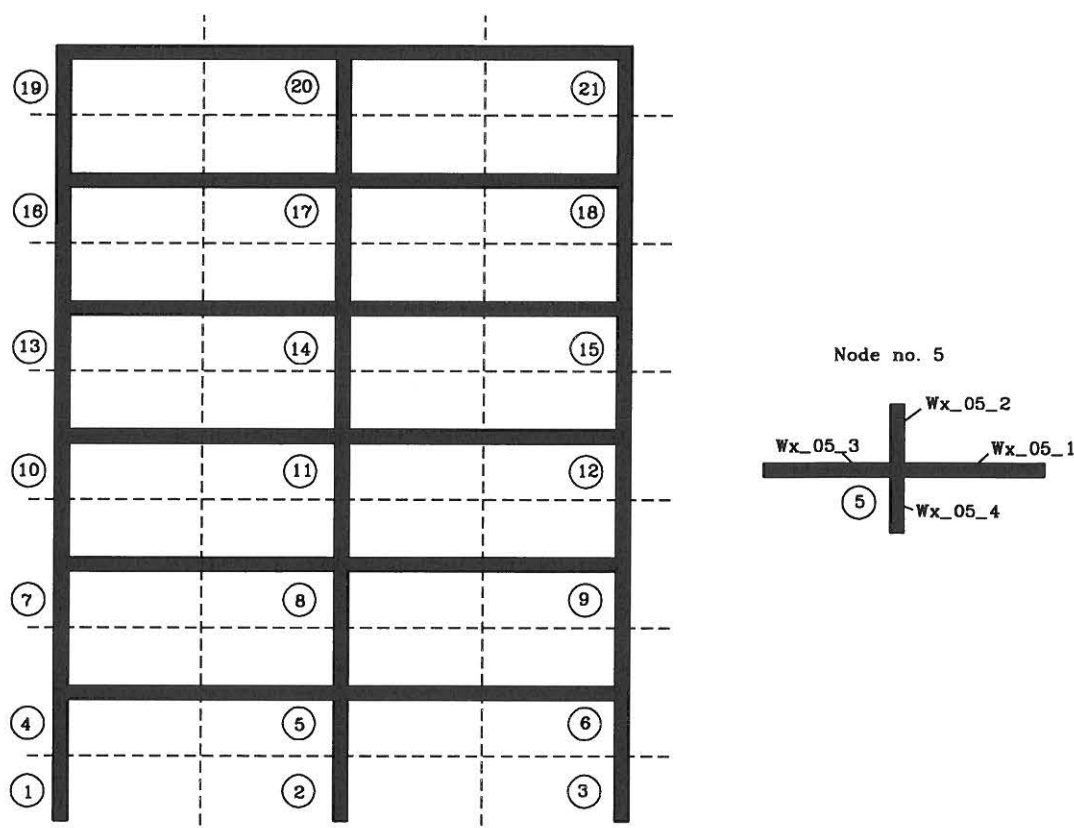
Figure 6.4: a) Cutting lines for separation of frames into smaller specimens for statical testing. b) labelling of the beams and columns at each node.

Due to symmetry only the outer columns and beams in one side of the frame and the center columns are tested.

A photo of the cutting process is shown in figure A.7.

6.2.2   Procedure for static tests on reference and damaged specimens

The static testing of the different beams and columns were performed using a schematical as shown in figure 6.5.
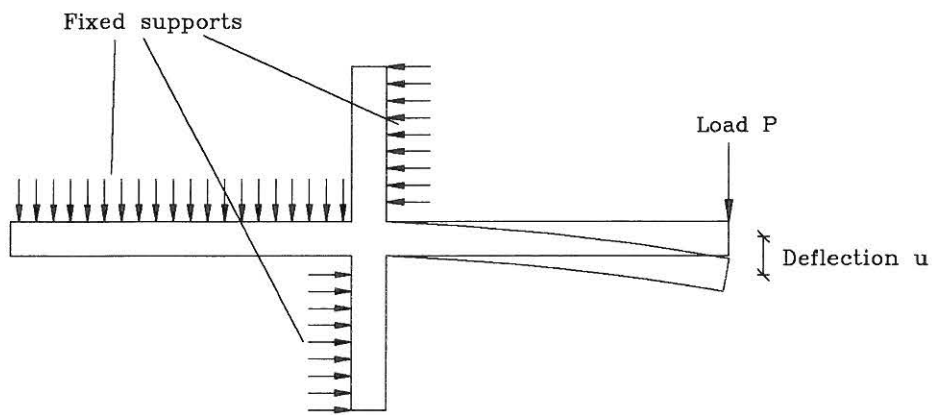
Figure 6.5: Schematical set-up of static testing of reference and damaged specimens.

A photo of the applied set-up are shown in figure A.8 and the data aquisition system in figure A.9.

6.2.3 Results of Static bending tests

The force-deformation curve obtained for each of the half-beams and half-columns are shown in figures 6.6-6.11.
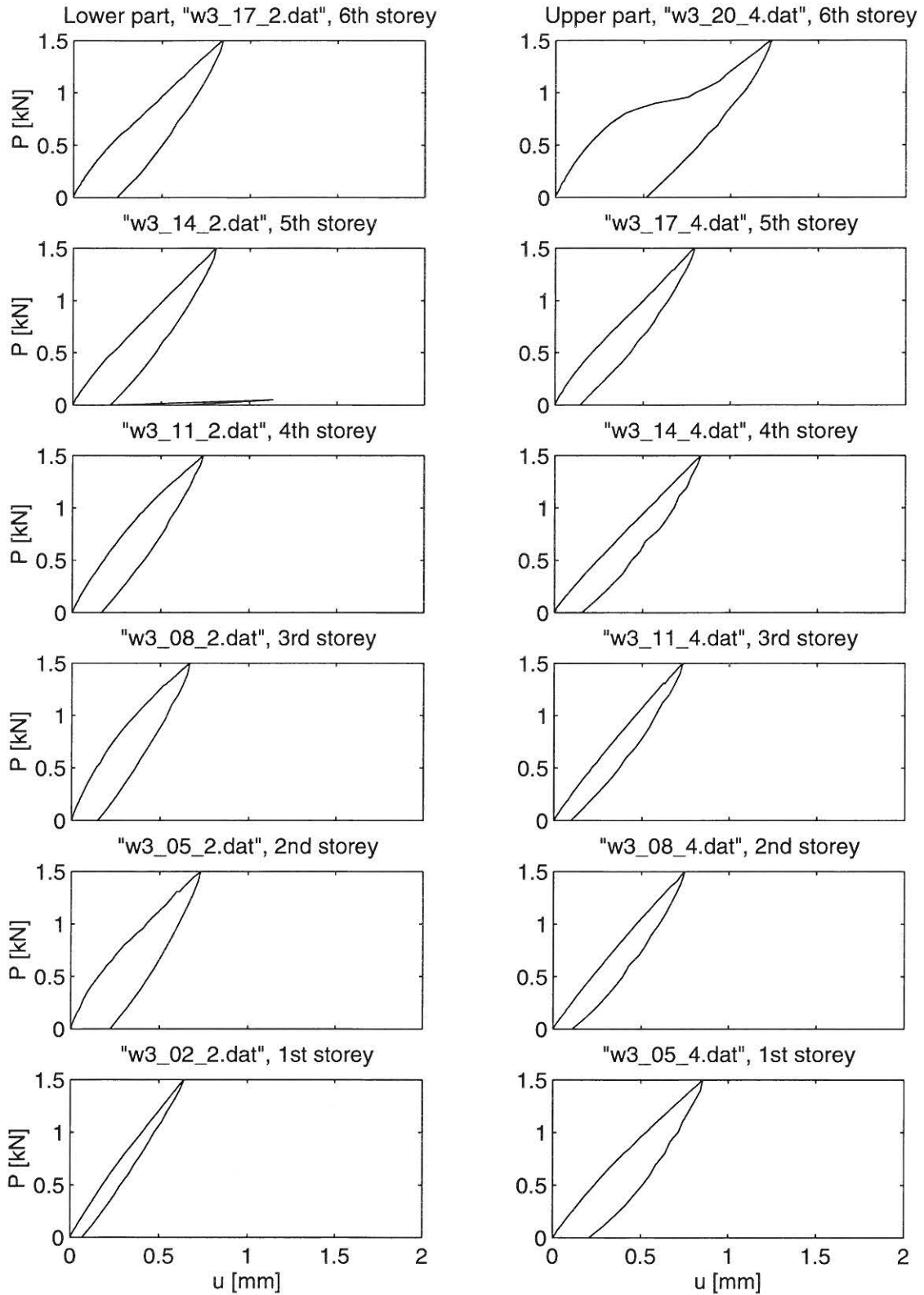
Figure 6.6: Force-deformation curves for the center columns obtained from the static tests. Undamaged frame AAUW3.
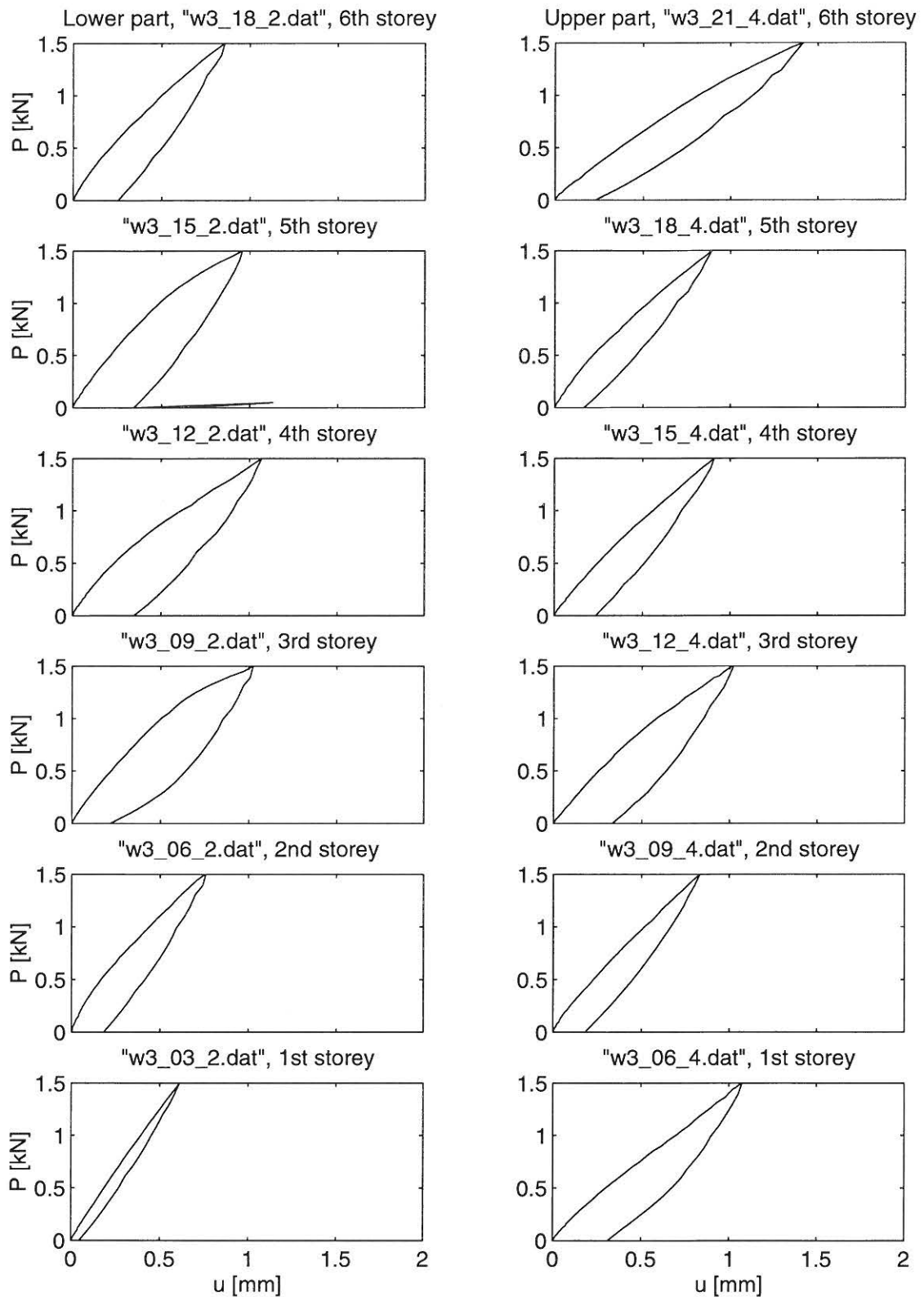
Figure 6.7: Force-deformation curves for the outer columns obtained from the static tests. Undamaged frame AAUW3.
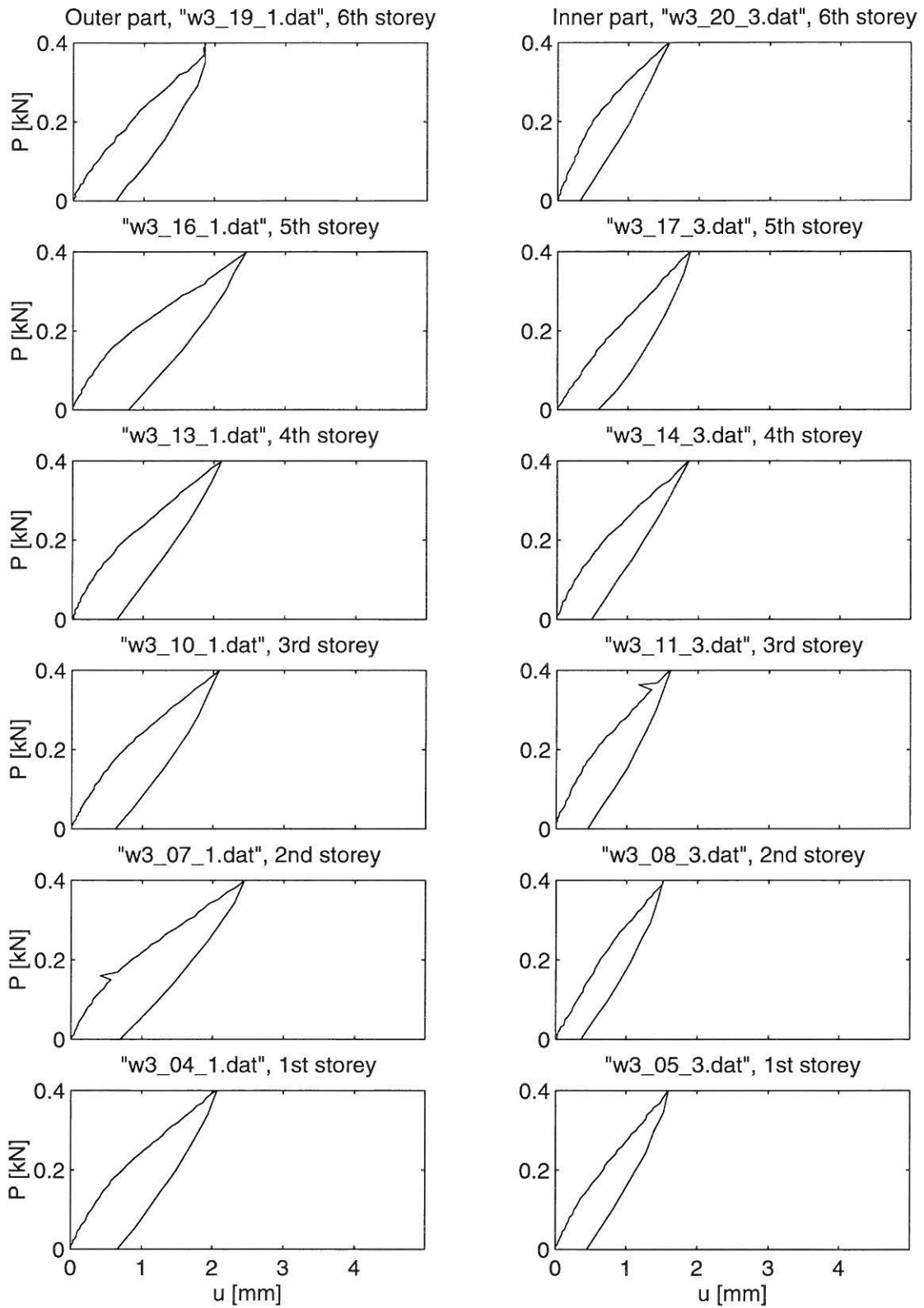
Figure 6.8: Force-deformation curves for the beams obtained from the static tests. Undamaged frame AAUW3.
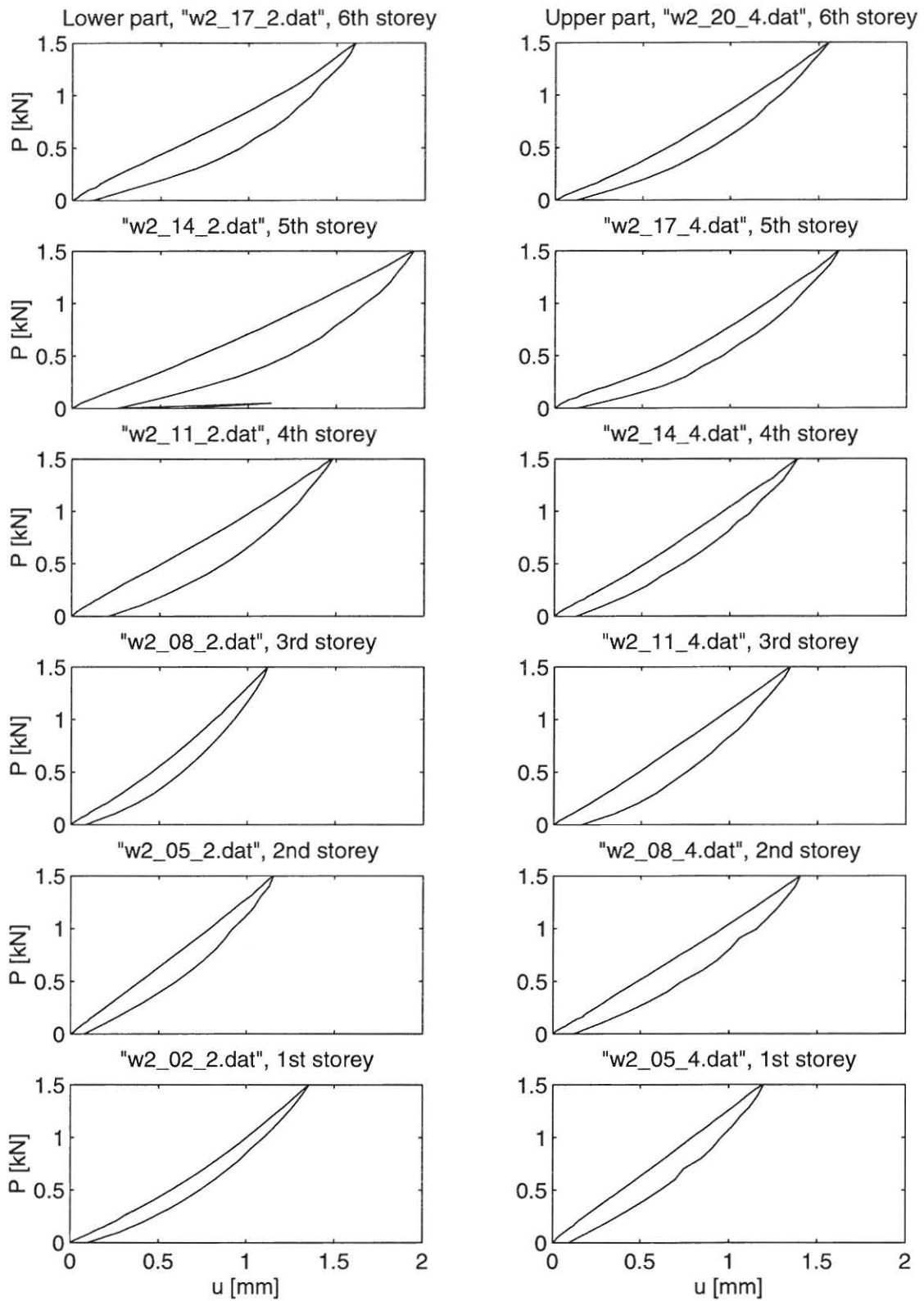
Figure 6.9: Force-deformation curves for the center columns obtained from the static tests. Damaged structure AAUW1.
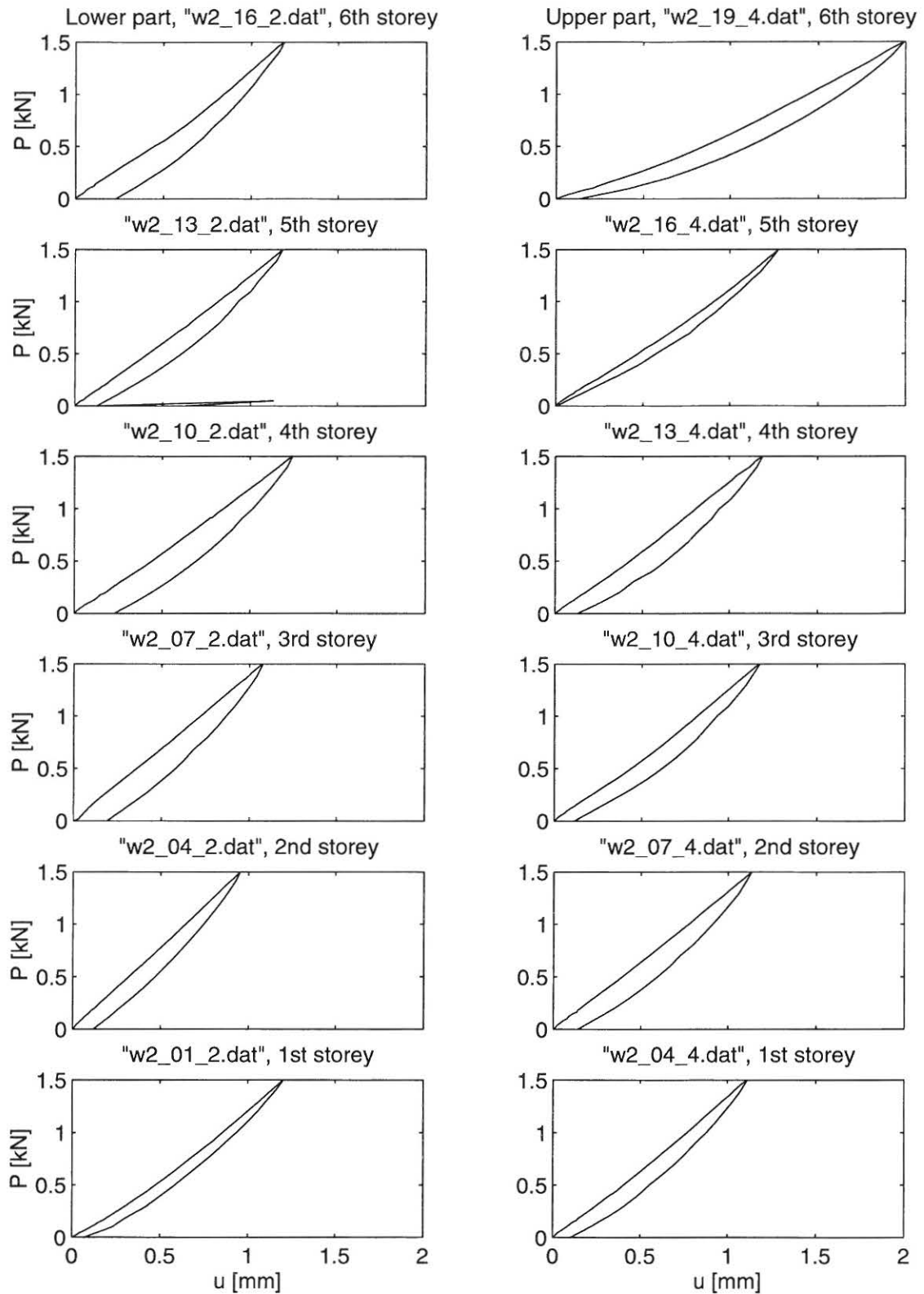
Figure 6.10: Force-deformation curves for the outer columns obtained from the static tests. Damaged structure AAUW1.

By comparing figures 6.6-6.8 with figures 6.9-6.11 a severe stiffness-reduction is seen i all elements. In general the largest reductions in stiffnesses are seen in the center columns at the first fourth and fifth storey.

It should be noted that during the test of beam "w3_20_4" sliding in the set-up occurred causing the large permanent deformations seen in the figure.

The data can be found in the files with names as marked on figures 6.6-6.11.
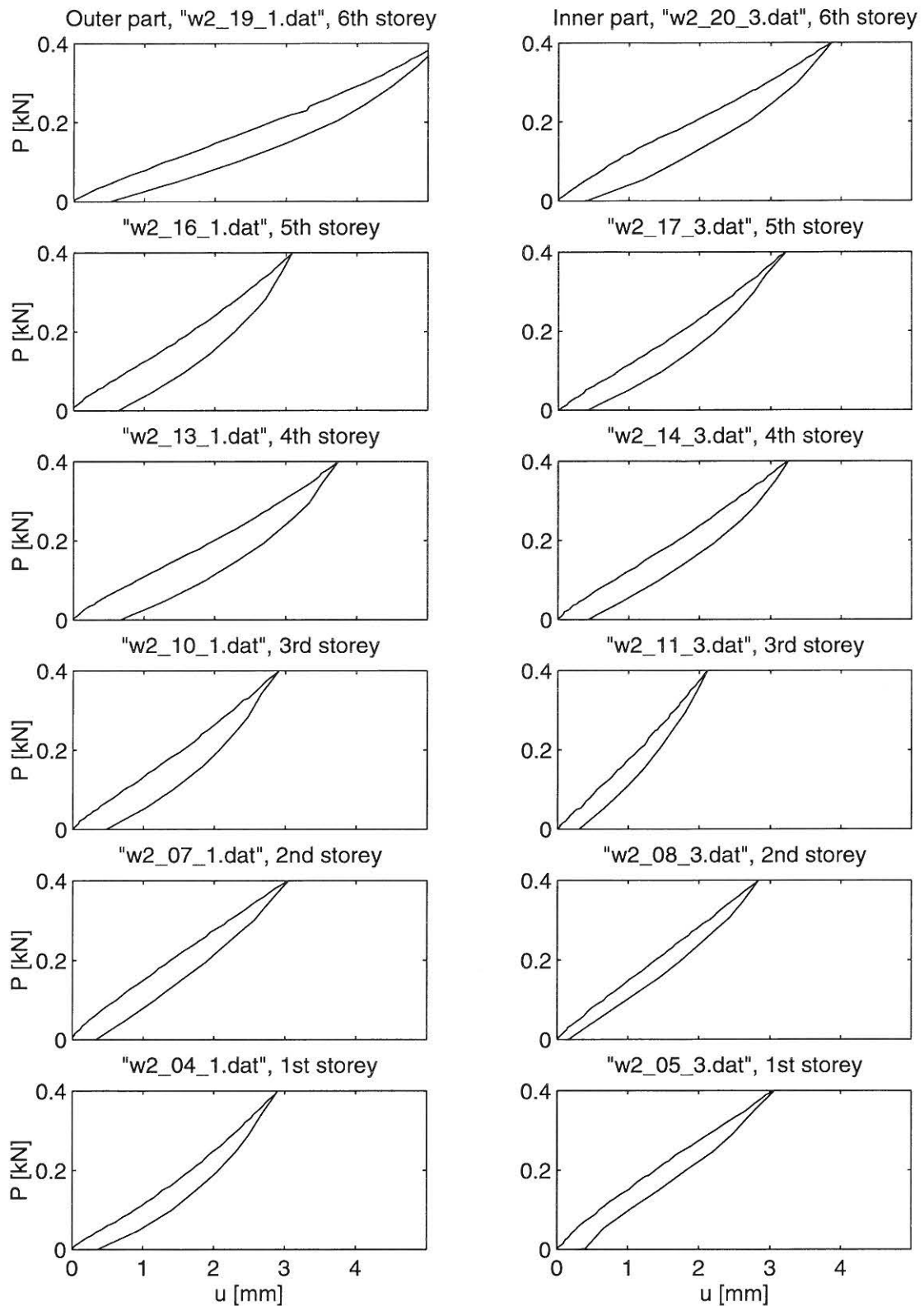
Figure 6.11: Force-deformation curves for the beams obtained from the static tests. Damaged structure AAUW1.

Chapter 7

Results of visual inspection after each run

After each of the strong motion loadings, the structure is visually examined by means of a magnification glass where all cracks were marked by different colors of pens respectively and photos were taken.

7.1 Definition of used classifications

After each series of strong motion loadings the structure was visually examined and the damage state of each storey of the building is classified into one of the following 6 classifications: Undamaged (U), Cracked (CR), Lightly Damaged (LD), Damaged (D), Severely Damaged (SD) or Collapse (CO). Each of the 6 classifications are defined in table 7.1.

Category	Definition
Undamaged UD	No external sign of changed integrity of any of the columns or beams in the storey
Cracked CR	Lightly cracking observed in several members but no permanent deformation
Lightly Dam. LD	Severe cracking observed with minor permanent deformations
Damaged D	Severe cracking and locally large permanent deformations observed.
Severely Dam. SD	Large permanent deformations observed and spalling of concrete at some members
Collapse CO	Very large permanent deformations observed and severe spalling of concrete at several members

Table 7.1: *Definition of the 6 damage classifications used.*

7.2 Damage Assessment of Frames AAUWa-b

Generally the cracks/damage were concentrated at the beam-column junctions at all load levels and the inspection was therefore concentrated at the nodes. After earthquake 1, (EQ1), the

inspection made on the nodes showed no serious cracks other than mostly micro-cracks. Only the nodes 2, 12 and 18 of frame AAUWb had shear-cracks of width not more than 0.02 mm. These cracks increased in length after EQ2 and also new shear cracks occured at the nodes 8 and 18 of frame AAUWa and 1, 8 and 15 of frame AAUWb. So the general impression from these visual inspections after EQ1 and EQ2 was that the damage was limited since only small cracks and some reasonable shear-cracks were present.

EQ3 resulted some heavy damages at the nodes of second and the fourth storeys which can be seen from the pictures in figure 7.1. Other than these heavy damages, most of the nodes had significant shear cracks. All three columns of the fourth storey of frame AAUWb had horizontal shear-cuts where the maximum shear force supposed to be. Storey 2 also had the same kind of damage.

There was not any total or partial collapse after any of the earthquake events. But the nodes 2, 11 and 14 of the frame AAUWa and the nodes 2, 11 and 14 of AAUWb can be presented as hinges. These visual inspections are collected together in the table 7.2 given below.

Storey	Frame	EQ1	EQ2	EQ3
1	AAUWa/AAUWb	UD/CR	CR/LD	SD/SD
2	AAUWa/AAUWb	UD/CR	CR/CR	LD/D
3	AAUWa/AAUWb	CR/UD	LD/CR	LD/D
4	AAUWa/AAUWb	CR/CR	CR/CR	SD/SD
5	AAUWa/AAUWb	UD/UD	CR/CR	SD/SD
6	AAUWa/AAUWb	UD/CR	CR/CR	CR/CR

Table 7.2: *Damage classifications after the three earthquake events for frame AAUW.*

It is quite clear from table 7.2 that first, fourth and the fifth storeys are the most damaged ones, while storey six has the least damage. Especially, the shear-cuts seen in all the three columns of the fourth storey, prove that the storey has weaker columns than the others and the columns are almost in the limit state of their bearing capacities.
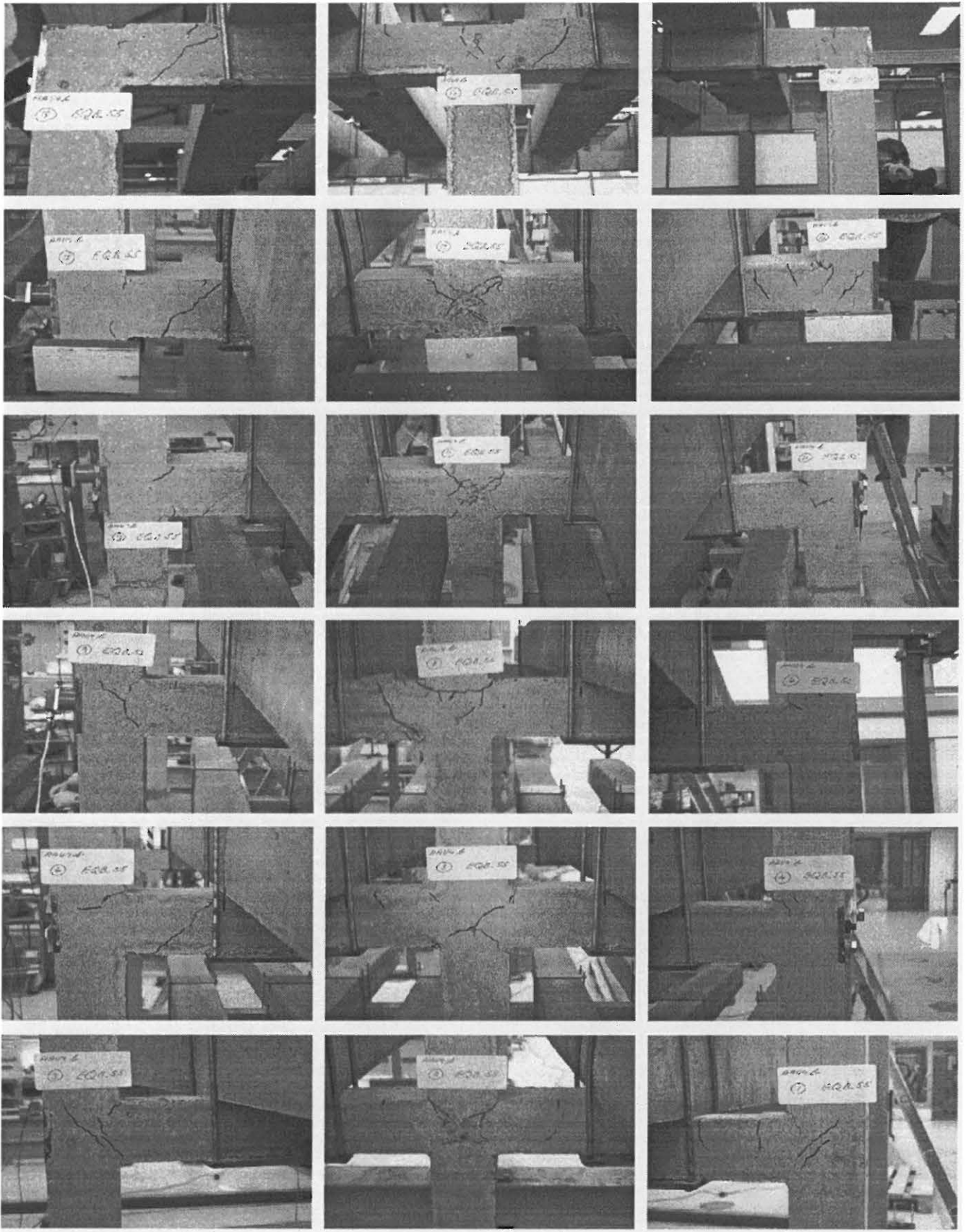
Figure 7.1: Photos of all nodes in frame AAUWb.

Chapter 8

Summary

In this report the results from a series of shaking table tests performed on a 6-storey model test RC-frame tested at the Structural laboratory at Aalborg University, Denmark are presented. The model test frame considered are designed with a weak fourth storey where the amount of reinforcement has been reduced and steel of a poorer quality has been used. The structure is instrumented with accelerometers at all storeys and at the shaking table. Before strong motion sequences are applied to the structure free decay tests are performed at different excitation levels to provide data for modal identification of the undamaged structure. Furthermore, static tests are performed where a definite force are applied at the top storey and the displacements were measured at the 6 storeys. Three sequences of strong motions of increasing magnitude were applied to the structure and acceleration time series at all storey were collected. In between the strong motion events and after the last one free decays as well as static tests were performed as for the undamaged structure. After each strong motion event all cracks were marked with pens of different colours and after the termination of the dynamic tests pictures were taken off all nodes, where the cracks were located. When the test structure was taken down one of the frames was cut into smaller specimens and each beam and column was statically tested in order to evaluate the reduced bending stiffness. These stiffnesses were compared to stiffnessess obtained from a reference frame.

Chapter 9

Acknowledgement

Bibliography

[1] Banon, H., Biggs, J. M. and Irvine, H. M., *Seismic Damage in Reinforced Concrete Frames.* Journal of the Structural Division, Proc., ASCE, Vol. 107, No. ST9, Sept. 1981, pp 1713-1729.

[2] Banon, H., and Veneziano, D., *Seismic Safety of Reinforced Concrete Members and Structures.* Earthquake Engineering and Structural Dynamics, Vol. 10, 1982, pp 179-193.

[3] Banon, H. *Prediction of Seismic Damage in Reinforced Concrete Frames.* Publication R80-16, Department of Civil Engineering, MIT, Cambridge Mass., May 1980.

[4] Beck, J.L. and Jennings, P.C., *Structural Identification using Linear Models and Earthquake Records.* Earthquake Engineering and Structural Dynamics, Vol. 8, 1980, pp. 145-160.

[5] Bracci, J.M. and Reinhorn, A.M., *Shaking Table Testing of a 1:3 scale RC Frame Model.* Proceedings of Structural Dynamics - EURODYN'96, Ed. Augusti, Borri and Spinelli, Torino, Italy, 1996, pp. 893-897.

[6] Casas, J.R. *Structural Damage Identification from Dynamic-Test Data.* ASCE J. Struc. Eng. Vol. 120, No. 8, Aug. 1994, pp. 2437-2450.

[7] Cecen, H., *Response of Ten Story, Reinforced Model Frames to Simulated Earthquakes.* Thesis presented to the University of Illinois, Urbana, I11., in partial fulfilment of the requirements for the degree of Doctor of Philosophy, 1979.

[8] DiPasquale, E. and Çakmak, A. Ş. *Detection of Seismic Structural Damage using Parameter-Based Global Damage Indices.* Probalistic Engineering Mechanics, Vol. 5, No. 2, pp. 60-65, 1990.

[9] DiPasquale, E. and Çakmak, A. Ş. *Damage Assesment from Earthquake Records.* Structures and Stochastic Methods, Elsevier, Amsterdam, pp. 123-138.

[10] DiPasquale, E. and Çakmak, A. Ş. *Seismic Damage Assessment using Linear Models.* Soil Dynamics and Earthquake Engineering, Vol. 9, No. 4, pp. 194-215, 1990.

[11] DiPasquale, E., Ju, J.-W., Askar, A. and Çakmak, A. Ş. *Relation Between Global Damage Indices and Local Stiffness Degradation.* Journal of Structural Engineering, Vol. 116, No. 5, pp. 1440-1456, 1990.

[12] Hassotis, S and Jeong, G.D. *Assessment of Structural Damage from Natural Frequency Measurements.* Computers and Structures, Vol. 49, No. 4, pp. 679-691, 1993.

[13] Hoshiya, M. and Saito, E. *Structural Identification by Extended Kalman Filter.* Journal of Engineering Mechanics, Vol. 110, No. 12, Dec. 1984.

[14] Kirkegaard, P.H. and Rytter, A. *Use of a Neural Network for Damage Detection in a Steel Member.* Presented at the third Int. Conf. in the Application of Artificial Intelligence to Civil Engineering Structures, Civil-Comp93, Edinburgh, August 17-19, 1993.

[15] Kirkegaard, P.H., Skjærbæk, P.S. and Andersen, P., *Identification of Time-Varying Civil Engineering Structures using Multivariate Recursive Time Domain Models.* Proceedings of the 21st international Symposium on Noise and Vibrations, ISMA21, Leuven, Belgium, September 18-20, 1996.

[16] Kirkegaard, P.H., Skjærbæk, P.S. and Nielsen, S.R.K., *Identification Report: !!!!.* Internal Laboratory Report, Aalborg University, Denmark, 1997.

[17] Koh, C.G., See, L.M. and Balendra, T. *Estimation of Structural Parameters in Time Domain: A Substructure Approach.* Earthquake Engineering and Structural Dynamics, Vol. 20, No. 8, pp. 787-801, Aug. 1991.

[18] Koh, C.G., See, L.M. and Balendra, T. *Damage Detection of Buildings: Numerical and Experimental studies.* ASCE J. Str.Eng., Vol. 121, No. 8, pp. 1155-1160, Aug. 1995.

[19] Köylüoğlu, H.U., Nielsen, S.R.K. and Çakmak, A.Ş., *Local and Modal Damage Indicators for Reinforced Concrete Shear Frames Subject to Earthquakes.* Submitted to Journal of Engineering Mechanics, ASCE, 1996.

[20] Köylüoğlu, H.U., Nielsen, S.R.K. and Çakmak, A.Ş., *Midbroken Reinforced Shear Frames due to Earthquakes. A Hysteretic Model to Quantify damage at the Storey Level.* Soil Dynamics and Earthquake Engineering, 16 (1997), pp. 95-112.

[21] Kratzig, W.B. *Seismic Damage Simulation: A Low-cycle fatigue Process.* Proceedings of Structural Dynamics - EURODYN'96, Ed. Augusti, Borri and Spinelli, Torino, Italy, 1996, pp. 15-22.

[22] Köylüoğlu, H. U., Nielsen, S. R. K., Çakmak, A.Ş. and Kirkegaard, P. H. *Prediction of Global and Localized Damage and Future Reliability for RC Structures subject to Earthquakes.* Structural Reliability Theory, paper 128, Aalborg University 1994 (submitted to Soil Dynamics and Earthquake Engineering).

[23] Nielsen, S.R.K., Köylüoğlu, H.U. and Çakmak, A.Ş., *One and Two-Dimensional Maximum Softening Damage Indicators for Reinforced Concrete Structures Under Seismic Excitation.* Soil Dynamics and Earthquake Engineering, 11, pp. 435-443, 1992.

[24] Nielsen, S.R.K. and Çakmak, A.Ş., *Evaluation of Maximum Softening Damage Indicator for Reinforced Concrete Under Seismic Excitation.* Proceedings of the First International Conference on Computional Stochastic Mechanics. Ed. Spanos and Brebbia, pp. 169-184, 1992.

[25] Pandey, A.K. and Biswas, M., *Damage Detection in Structures using Changes in Flexibility.* Journal of Sound and Vibration 169(1), pp. 3-17, 1994.

[26] Park, Y.J. and Ang, A. H.-S., *Mechanistic Seismic Damage Model for Reinforced Concrete.* ASCE J. Struc. Eng., 111(4) April 1985, pp.722-739.

[27] Park, Y.J., Ang, A. H.-S., and Wen, Y.K., *Seismic Damage Analysis of Reinforced Concrete Buildings.* ASCE J. Struc. Eng., 111 (4) April 1985, pp. 740-757.

[28] Park, Y.J., Ang, A. H.-S., and Wen, Y.K., *Damage Limiting Aseismic Design of Buildings.* Earthquake Spectra, Vol. 3 No. 1, Feb. 1987, pp. 1-26.

[29] Park, Y.S., Park, H.S., and Lee, S.S., *Weighted-Error-Matrix Application to Detect Stiffness Damage by Dynamic-Characteristic Measurement.* Journal of Modal Analysis, July. 1988, pp. 101-107.

[30] Penny, J.E.T., Wilson, D.A.L., and Friswell, M.I., *Damage Location in Structures using Vibration Data.* Aston University, Birmingham, UK, 1993.

[31] Reinhorn, A.M., Seidel, M.J., Kunnath, S.K. and Park, Y.J., *Damage Assessment of Reinforced Concrete Structures in Eastern United States.* NCEER-88-0016 technical report, June 1988.

[32] Rodriguez-Gomez, S., *Evaluation of Seismic Damage Indices for Reinforced Concrete Structures.* M.Sc. Thesis, Princeton University, Oct. 1990.

[33] Ruiz, P. and Penzien, J., *Probabilistic Study of Behaviour of Structures during Earthquakes.* Report No. EERC 69-3, University of California, Berkeley, California, USA.

[34] Rytter, A. *Vibration Based Inspection of Civil Engineering Structures.* Ph.D. Thesis, Aalborg University, 1993.

[35] Seible, F., Hegenmier, G.A., Igarashi, A. and Kingsley, G.R., *Simulated Seismic-Load Tests on Full-Scale Five-Story Masonry Building.* ASCE J. Struc. Eng., Vol. 120, No. 3, March 1994, pp. 903-923.

[36] Shah, P.C. and Udwadia, F.E., *A Methodology for Optimal Sensor Locations for Identification of Dynamic Systems.* Journal of Applied Mechanics, Vol. 45, March 1978, pp. 188-196.

[37] Skjærbæk, P.S., Çakmak, A.S., Nielsen, S.R.K. and Çakmak, A.S., *Identification of Damage in RC-Structures from Earthquake Records - Optimal Location of Sensors* Fracture and Dynamics, Paper 77. Journal of Soil Dynamics and Earthquake Engineering, No. 15 , 1996, pp. 347-358.

[38] Skjærbæk, P.S., Nielsen, S.R.K. and Çakmak, A.S., *Damage Localization of Severely Damaged RC-structures based on Measured Eigenperiods from a Single Response.* Proceedings of the 4th International Conference on Localized Damage 96, June 3-5 1996, Fukuoka, Japan, pp. 815-822.

[39] Skjærbæk, P.S., Nielsen, S.R.K. and Çakmak, A.S., *Assessment of Damage in Seismically Excited RC-structures from a Single Measured Response* Proceedings of the 14th IMAC, Dearborn, Michigan, USA, February 12-15, 1996, pp. 133-139.

[40] Skjærbæk, P.S., *Damage Assessment of RC-Structures subject to Earthquakes*, Ph.D. thesis, Aalborg University, Denmark, 1997. Fracture and Dynamics, Paper No. 90.

[41] Skjærbæk, P.S., Kirkegaard, P.H. and Nielsen, S.R.K., *Experimental Case Study of Local Damage Indicators for a 2-bay, 6-Storey RC-Frame Subject to Earthquake.* Proceedings of the 15th International Modal Analysis Conference, February 3-6 1997, Orlando, Florida, USA.

[42] Stephens, J.E. and Yao, J.P.T., *Damage Assesment Using Response Measurements.* ASCE J. Struc. Eng. 113 (4) April 1987, pp. 787-801.

[43] Stephens, J.E., *Structural Damage Assesment Using Response Measurements.* Ph.D.-thesis, Purdue University, 1985.

[44] Stubbs, N. and Osegueda, R., *Damage Detection in Periodic Structures.* Damage Mechanics and Continuum Mechanics, ASCE, October 1985.

[45] Tajimi, H., *Semi-Empirical Formula for the Seismic Characteristics of the Ground.* Proceedings of the 2nd World Conference on Earthquake Engineering, Vol. II, 781-798, Tokyo and Kyoto, 1960.

[46] Vestroni F., Cerri, M.N. and Antonacci, E., *Damage Detection in Vibrating Structures.* Proceedings of Structural Dynamics - EURODYN'96, Ed. Augusti, Borri and Spinelli, Torino, Italy, 1996, pp. 41-50.

Appendix A

Photos

In this appendix photos taken during the process of construction and testing of the frames.

A.1 The construction process

Figure A.1: The form used for construction of the frames.
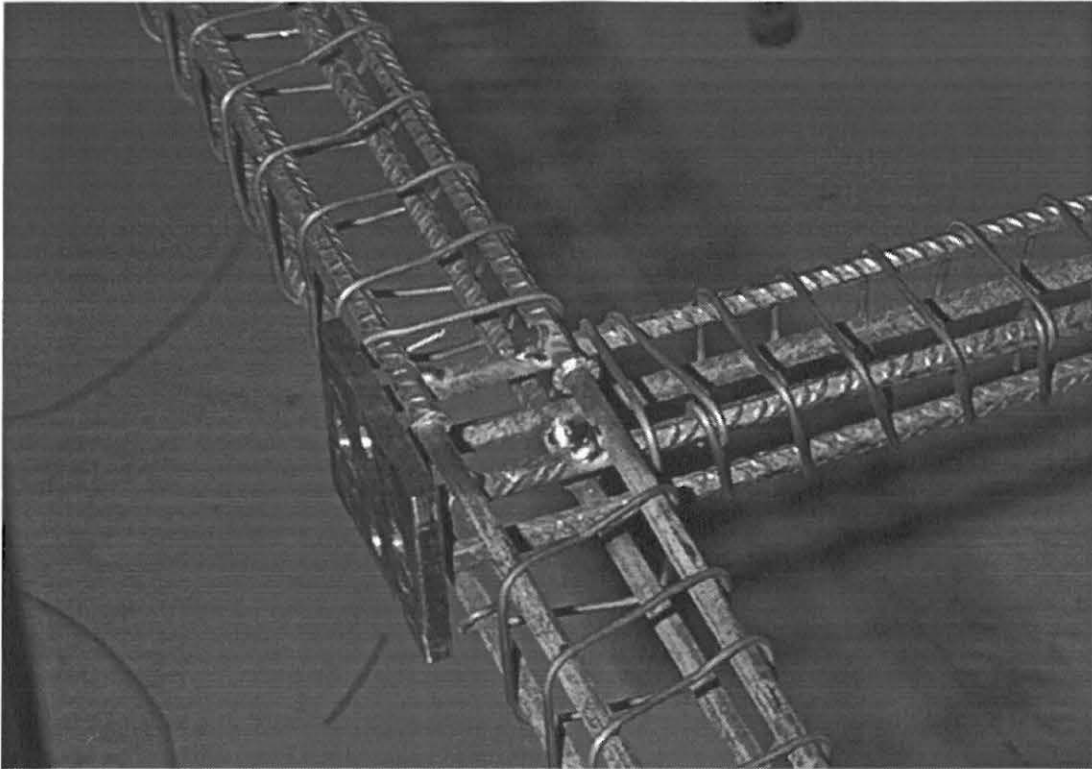
Figure A.2: Detail showing stuk-welding of reinforcement.
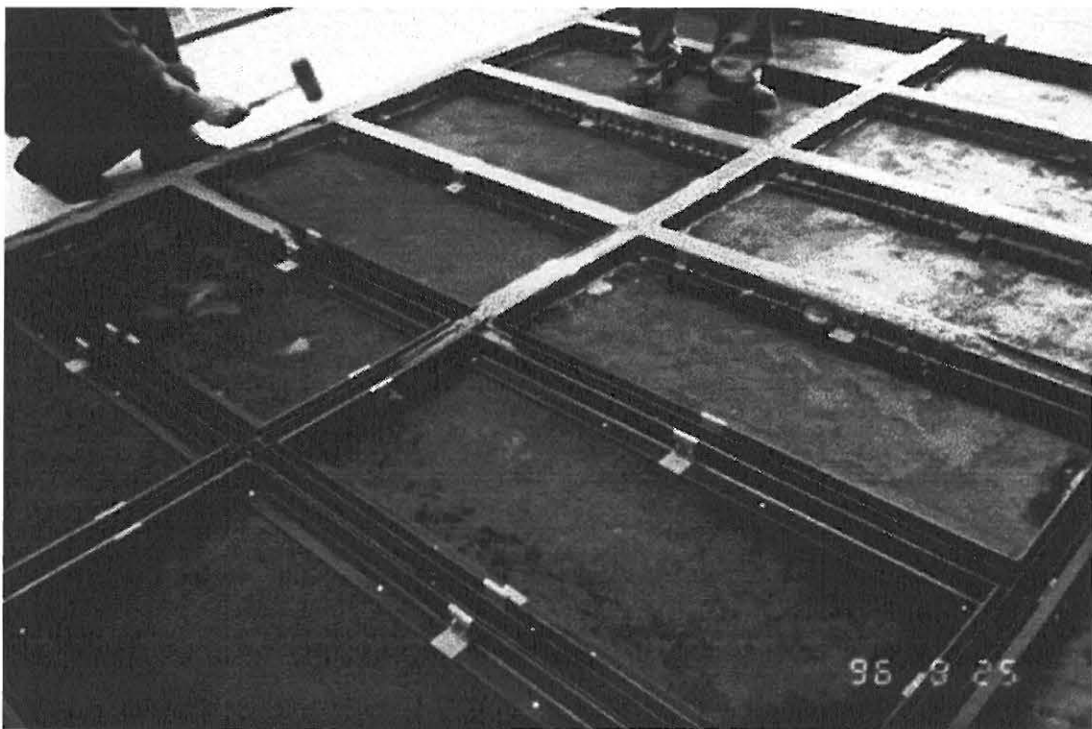
Figure A.3: Pouring and vibration of concrete.
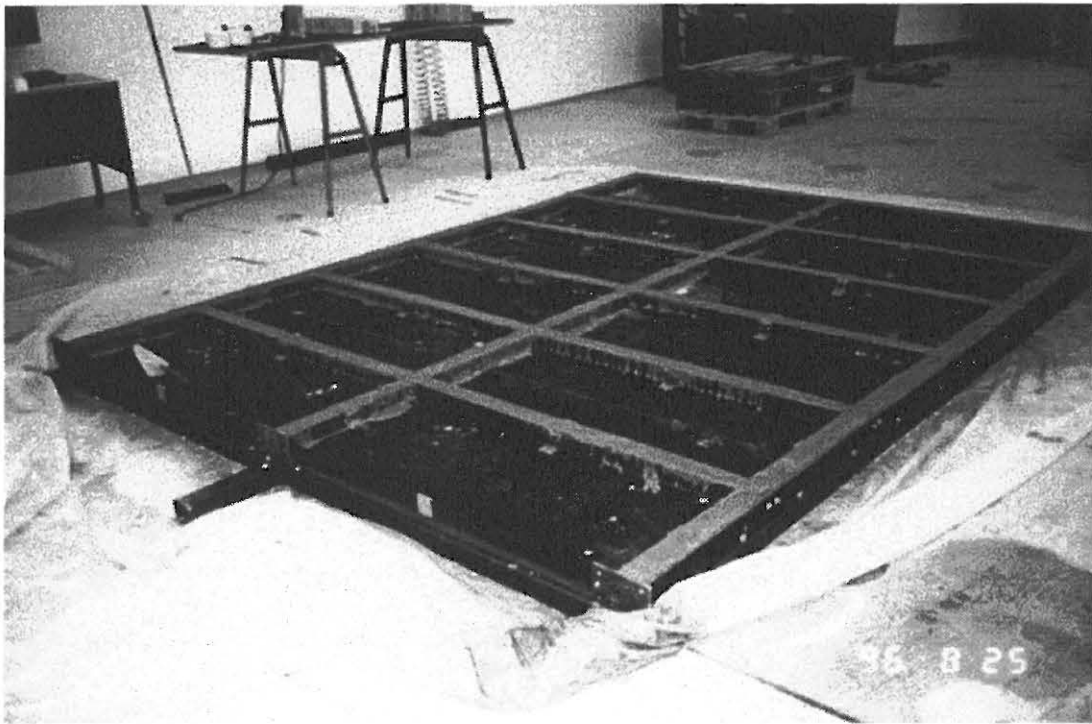
Figure A.4: The frame and form after pouring and vibrating of concrete.

Figure A.5: Data aquisition system.

Figure A.6: Undamaged structure before testing.

A.2 Static Testing
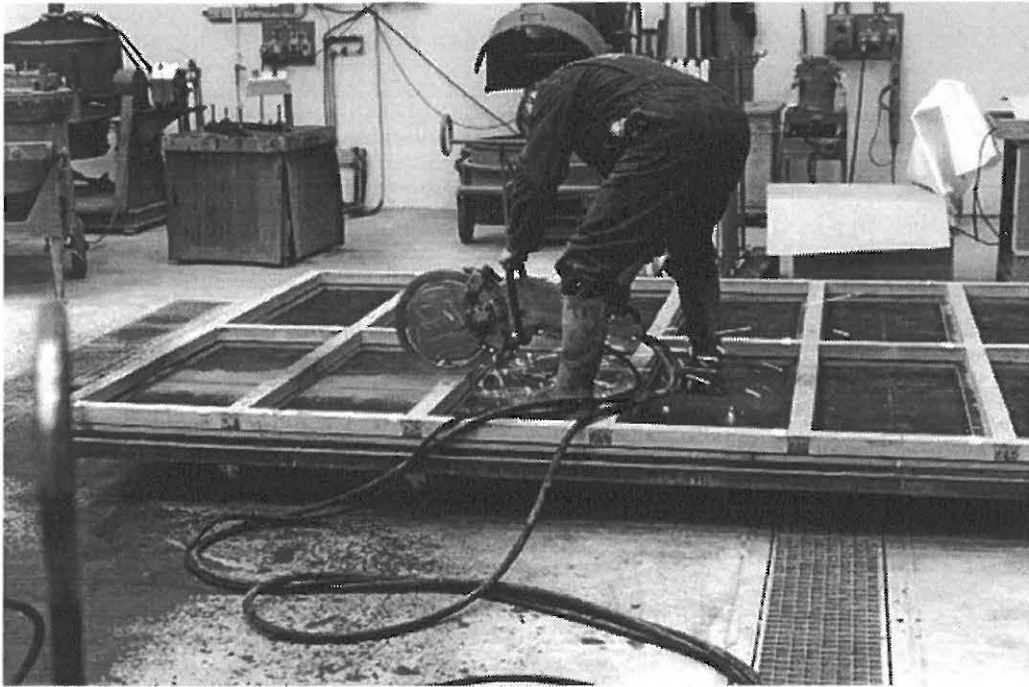
Figure A.7: Photo of the cutting.
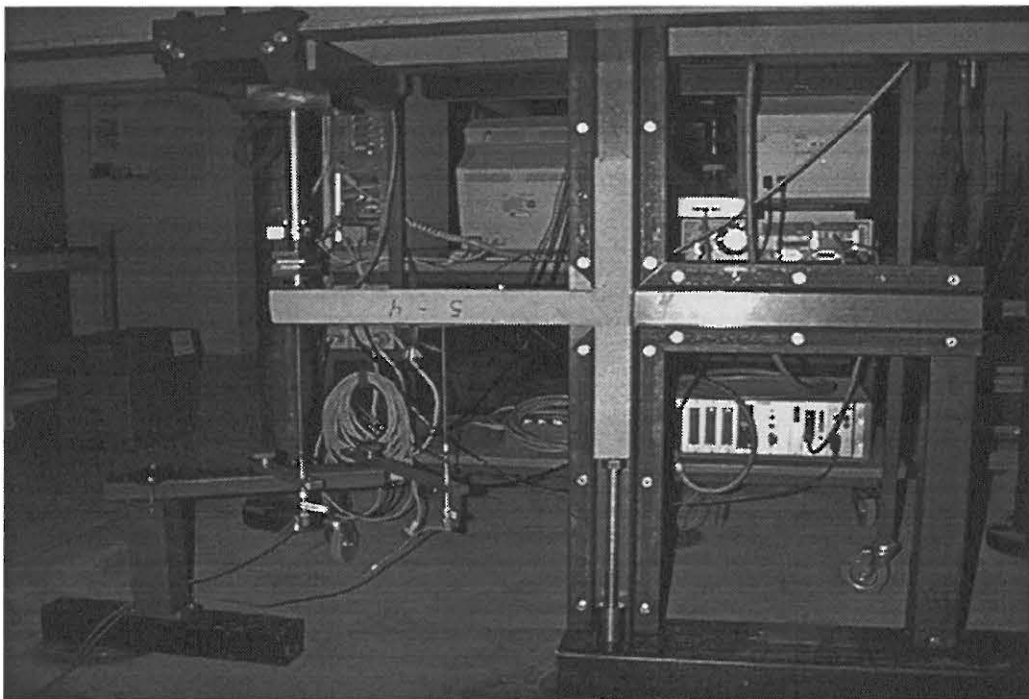
Figure A.8: Photo of the static test setup used for testing structural components.

Figure A.9: Photo of the data acqusition system used for the static tests of parts of the structure.

Appendix B

File Data Sheets

In this appendix the data sheets of all files are listed with all calibration factors, date of tests etc.

Data sheet no. 1.

Frame:	AAU-W
Date:	040397
Sampling rate:	150 Hz
Number of points:	5000

Valid for the files:	
	fd4_b01.dat
	fd4_b02.dat
	fd4_b03.dat
	fd4_b04.dat

Ch.	Amp.	LFL	UFL	Comments
1	10 V/63kN	-	-	
2	10 V/20mm	-	-	
3	0.1 V/ms^{-2}	-	-	BK8306
4	0.1 V/ms^{-2}	-	-	BK8306
5	0.1 V/ms^{-2}	0.2 Hz	1 kHz	BK4370
6	0.1 V/ms^{-2}	0.2 Hz	1 kHz	BK4370
7	0.1 V/ms^{-2}	0.2 Hz	1 kHz	BK4370
8	0.1 V/ms^{-2}	0.2 Hz	1 kHz	BK4370
9	0.1 V/ms^{-2}	0.2 Hz	1 kHz	BK4370
10	-	-	-	-
11	1.027 V/ms^{-2}	-	-	K8304B2
12	0.963 V/ms^{-2}	-	-	K8304B2
13	0.956 V/ms^{-2}	-	-	K8304B2
14	1.008 V/ms^{-2}	-	-	K8304B2
15	0.963 V/ms^{-2}	-	-	K8304B2
16	0.963 V/ms^{-2}	-	-	K8304B2

Table B.1: *Data sheet 1.*

Data sheet no. 2.

Frame:	AAU-W
Date:	050397
Sampling rate:	150 Hz
Number of points:	5000 or 6000

Valid for the files:	
	fd4_b05.dat
	sm4_20b.dat
	fd4_b06.dat
	fd4_b07.dat
	fd4_b08.dat

Ch.	Amp.	LFL	UFL	Comments
1	10 V/63kN	-	-	
2	10 V/20mm	-	-	
3	0.1 V/ms^{-2}	-	-	BK8306
4	0.1 V/ms^{-2}	-	-	BK8306
5	0.1 V/ms^{-2}	0.2 Hz	1 kHz	BK4370
6	0.1 V/ms^{-2}	0.2 Hz	1 kHz	BK4370
7	0.1 V/ms^{-2}	0.2 Hz	1 kHz	BK4370
8	0.1 V/ms^{-2}	0.2 Hz	1 kHz	BK4370
9	0.1 V/ms^{-2}	0.2 Hz	1 kHz	BK4370
10	-	-	-	-
11	1.027 V/ms^{-2}	-	-	K8304B2
12	0.963 V/ms^{-2}	-	-	K8304B2
13	0.956 V/ms^{-2}	-	-	K8304B2
14	1.008 V/ms^{-2}	-	-	K8304B2
15	0.963 V/ms^{-2}	-	-	K8304B2
16	0.963 V/ms^{-2}	-	-	K8304B2

Table B.2: *Data sheet 2.*

Data sheet no. 3.

Frame:	AAU-W
Date:	060397
Sampling rate:	150 Hz
Number of points:	5000 or 6000

Valid for the files:	
	fd4_b09.dat
	sm4_40b.dat
	fd4_b10.dat
	fd4_b11.dat
	fd4_b12.dat

Ch.	Amp.	LFL	UFL	Comments
1	10 V/63kN	-	-	
2	10 V/20mm	-	-	
3	0.1 V/ms^{-2}	-	-	BK8306
4	0.1 V/ms^{-2}	-	-	BK8306
5	0.1 V/ms^{-2}	0.2 Hz	1 kHz	BK4370
6	0.1 V/ms^{-2}	0.2 Hz	1 kHz	BK4370
7	0.1 V/ms^{-2}	0.2 Hz	1 kHz	BK4370
8	0.1 V/ms^{-2}	0.2 Hz	1 kHz	BK4370
9	0.1 V/ms^{-2}	0.2 Hz	1 kHz	BK4370
10	-	-	-	-
11	1.027 V/ms^{-2}	-	-	K8304B2
12	0.963 V/ms^{-2}	-	-	K8304B2
13	0.956 V/ms^{-2}	-	-	K8304B2
14	1.008 V/ms^{-2}	-	-	K8304B2
15	0.963 V/ms^{-2}	-	-	K8304B2
16	0.963 V/ms^{-2}	-	-	K8304B2

Table B.3: *Data sheet 3.*

Data sheet no. 4.

Frame:	AAU-W
Date:	070397
Sampling rate:	150 Hz
Number of points:	5000 or 6000

Valid for the files:	
	fd4_b13.dat
	sm4_55b.dat
	fd4_b14.dat
	fd4_b15.dat
	fd4_b16.dat

Ch.	Amp.	LFL	UFL	Comments
1	10 V/63kN	-	-	
2	10 V/20mm	-	-	
3	0.1 V/ms^{-2}	-	-	BK8306
4	0.1 V/ms^{-2}	-	-	BK8306
5	0.1 V/ms^{-2}	0.2 Hz	1 kHz	BK4370
6	0.1 V/ms^{-2}	0.2 Hz	1 kHz	BK4370
7	0.1 V/ms^{-2}	0.2 Hz	1 kHz	BK4370
8	0.1 V/ms^{-2}	0.2 Hz	1 kHz	BK4370
9	0.1 V/ms^{-2}	0.2 Hz	1 kHz	BK4370
10	-	-	-	-
11	1.027 V/ms^{-2}	-	-	K8304B2
12	0.963 V/ms^{-2}	-	-	K8304B2
13	0.956 V/ms^{-2}	-	-	K8304B2
14	1.008 V/ms^{-2}	-	-	K8304B2
15	0.963 V/ms^{-2}	-	-	K8304B2
16	0.963 V/ms^{-2}	-	-	K8304B2

Table B.4: *Data sheet 4.*

FRACTURE AND DYNAMICS PAPERS

PAPER NO. 64: P. S. Skjærbæk, S. R. K. Nielsen, A. Ş. Çakmak: *Assessment of Damage in Seismically Excited RC-Structures from a Single Measured Response.* ISSN 1395-7953 R9528.

PAPER NO. 65: J. C. Asmussen, S. R. Ibrahim, R. Brincker: *Random Decrement and Regression Analysis of Traffic Responses of Bridges.* ISSN 1395-7953 R9529.

PAPER NO. 66: R. Brincker, P. Andersen, M. E. Martinez, F. Tallavó: *Modal Analysis of an Offshore Platform using Two Different ARMA Approaches.* ISSN 1395-7953 R9531.

PAPER NO. 67: J. C. Asmussen, R. Brincker: *Estimation of Frequency Response Functions by Random Decrement.* ISSN 1395-7953 R9532.

PAPER NO. 68: P. H. Kirkegaard, P. Andersen, R. Brincker: *Identification of an Equivalent Linear Model for a Non-Linear Time-Variant RC-Structure.* ISSN 1395-7953 R9533.

PAPER NO. 69: P. H. Kirkegaard, P. Andersen, R. Brincker: *Identification of the Skirt Piled Gullfaks C Gravity Platform using ARMAV Models.* ISSN 1395-7953 R9534.

PAPER NO. 70: P. H. Kirkegaard, P. Andersen, R. Brincker: *Identification of Civil Engineering Structures using Multivariate ARMAV and RARMAV Models.* ISSN 1395-7953 R9535.

PAPER NO. 71: P. Andersen, R. Brincker, P. H. Kirkegaard: *Theory of Covariance Equivalent ARMAV Models of Civil Engineering Structures.* ISSN 1395-7953 R9536.

PAPER NO. 72: S. R. Ibrahim, R. Brincker, J. C. Asmussen: *Modal Parameter Identification from Responses of General Unknown Random Inputs.* ISSN 1395-7953 R9544.

PAPER NO. 73: S. R. K. Nielsen, P. H. Kirkegaard: *Active Vibration Control of a Monopile Offshore Structure. Part One - Pilot Project.* ISSN 1395-7953 R9609.

PAPER NO. 74: J. P. Ulfkjær, L. Pilegaard Hansen, S. Qvist, S. H. Madsen: *Fracture Energy of Plain Concrete Beams at Different Rates of Loading.* ISSN 1395-7953 R9610.

PAPER NO 75: J. P. Ulfkjær, M. S. Henriksen, B. Aarup: *Experimental Investigation of the Fracture Behaviour of Reinforced Ultra High Strength Concrete.* ISSN 1395-7953 R9611.

PAPER NO. 76: J. C. Asmussen, P. Andersen: *Identification of EURO-SEIS Test Structure.* ISSN 1395-7953 R9612.

PAPER NO. 77: P. S. Skjærbæk, S. R. K. Nielsen, A. Ş. Çakmak: *Identification of Damage in RC-Structures from Earthquake Records - Optimal Location of Sensors.* ISSN 1395-7953 R9614.

PAPER NO. 78: P. Andersen, P. H. Kirkegaard, R. Brincker: *System Identification of Civil Engineering Structures using State Space and ARMAV Models.* ISSN 1395-7953 R9618.

PAPER NO. 79: P. H. Kirkegaard, P. S. Skjærbæk, P. Andersen: *Identification of Time Varying Civil Engineering Structures using Multivariate Recursive Time Domain Models.* ISSN 1395-7953 R9619.

PAPER NO. 80: J. C. Asmussen, R. Brincker: *Estimation of Correlation Functions by Random Decrement.* ISSN 1395-7953 R9624.

FRACTURE AND DYNAMICS PAPERS

PAPER NO. 81: M. S. Henriksen, J. P. Ulfkjær, R. Brincker: *Scale Effects and Transitional Failure Phenomena of Reinforced concrete Beams in Flexure. Part 1.* ISSN 1395-7953 R9628.

PAPER NO. 82: P. Andersen, P. H. Kirkegaard, R. Brincker: *Filtering out Environmental Effects in Damage Detection of Civil Engineering Structures.* ISSN 1395-7953 R9633.

PAPER NO. 83: P. S. Skjærbæk, S. R. K. Nielsen, P. H. Kirkegaard, A. Ş. Çakmak: *Case Study of Local Damage Indicators for a 2-Bay, 6-Storey RC-Frame subject to Earthquakes.* ISSN 1395-7953 R9639.

PAPER NO. 84: P. S. Skjærbæk, S. R. K. Nielsen, P. H. Kirkegaard, A. Ş. Çakmak: *Modal Identification of a Time-Invariant 6-Storey Model Test RC-Frame from Free Decay Tests using Multi-Variate Models.* ISSN 1395-7953 R9640.

PAPER NO. 85: P. H. Kirkegaard, P. S. Skjærbæk, S. R. K. Nielsen: *Identification Report: Earthquake Tests on 2-Bay, 6-Storey Scale 1:5 RC-Frames.* ISSN 1395-7953 R9703.

PAPER NO. 86: P. S. Skjærbæk, S. R. K. Nielsen, P. H. Kirkegaard: *Earthquake Tests on Scale 1:5 RC-Frames.* ISSN 1395-7953 R9713.

PAPER NO. 89: P. S. Skjærbæk, P. H. Kirkegaard, S. R. K. Nielsen: *Shaking Table Tests of Reinforced Concrete Frames.* ISSN 1395-7953 R9704.

PAPER NO. 91: P. S. Skjærbæk, P. H. Kirkegaard, G. N. Fouskitakis, S. D. Fassois: *Non-Stationary Modelling and Simulation of Near-Source Earthquake Ground Motion: ARMA and Neural Network Methods.* ISSN 1395-7953 R9641.

PAPER NO. 92: J. C. Asmussen, S. R. Ibrahim, R. Brincker: *Application of Vector Triggering Random Decrement.* ISSN 1395-7953 R9634.

PAPER NO. 93: S. R. Ibrahim, J. C. Asmussen, R. Brincker: *Theory of Vector Triggering Random Decrement.* ISSN 1395-7953 R9635.

PAPER NO. 94: R. Brincker, J. C. Asmussen: *Random Decrement Based FRF Estimation.* ISSN 1395-7953 R9636.

PAPER NO. 95: P. H. Kirkegaard, P. Andersen, R. Brincker: *Structural Time Domain Identification (STDI) Toolbox for Use with MATLAB.* ISSN 1395-7953 R9642.

PAPER NO. 96: P. H. Kirkegaard, P. Andersen: *State Space Identification of Civil Engineering Structures from Output Measurements.* ISSN 1395-7953 R9643.

PAPER NO. 97: P. Andersen, P. H. Kirkegaard, R. Brincker: *Structural Time Domain Identification Toolbox - for Use with MATLAB.* ISSN 1395-7953 R9701.

PAPER NO. 98: P. S. Skjærbæk, B. Taşkin, S. R. K. Nielsen, P. H. Kirkegaard: *An Experimental Study of a Midbroken 2-Bay, 6-Storey Reinforced Concrete Frame subject to Earthquakes.* ISSN 1395-7953 R9706.

PAPER NO. 99: PAPER NO. 98: P. S. Skjærbæk, S. R. K. Nielsen, P. H. Kirkegaard, B. Taşkin: *Earthquake Tests on Midbroken Scale 1:5 Reinforced Concrete Frames.* ISSN 1395-7953 R9712.